Landscape ~~structure and rainstorms swing~~structures regulate the contrasting response of recession ~~nonlinearity~~along rainfall amounts

Jun-Yi Lee[1,2], Ci-Jian Yang[2,3], Tsung-Ren Peng[1], Tsung-Yu Lee[4], Jr-Chuan Huang[2]

[1]Department of Soil and Environmental Sciences, National Chung Hsing University, Taichung 402202, Taiwan
5 [2]Department of Geography, National Taiwan University, Taipei 106319, Taiwan
[3]German Research Centre for Geosciences (GFZ), Telegrafenberg, Potsdam 14473, Germany.
[4]Department of Geography, National Taiwan Normal University, Taipei 106209, Taiwan

Correspondence to: Jr-Chuan Huang(riverhuang@ntu.edu.tw)

Abstract. Streamflow recession discloses hydrological functioning, runoff dynamics, and storage status within catchments.
10 Understanding recession response to landscape ~~structure~~structures and rainstorms can be a guidance for assessing streamflow change under climate change. Yet, the documented response direction of recession is inconsistent and diverse. This study tested how landscape ~~structure~~structures and rainstorms regulate the response direction. We derived ~~260~~a total of 291 pairs of recession ~~rate~~coefficient, a, and nonlinearity, b, from power-law recession ($-dQ/dt = aQ^b$) ~~in~~over all 19 subtropical catchments with a broad rainfall spectrum. Results showed that the recession ~~rate~~coefficient increases with the drainage density and L/G
15 (the ratio (of flow-path length ~~over~~to gradient), particularly in small catchments, indicating that ~~the~~ catchments with the dense network ~~or~~ more short-and-gentle hillslopes would result in high ~~rates~~values of a. Apart from landscape structure, the ~~rate surprisingly~~a decreases with rainfall amount particularly in low L/G catchments. Probably because rainstorm facilitates connectivity in the saturated zones, which might conjoin more water from slow reservoirs and thus water drains slowly. Additionally, ~~the recession~~ nonlinearity increases with ~~spatial heterogeneity (drainage area)~~rainfall amount in larger
20 catchments but decreases ~~with hillslope hydraulics (drainage density).~~in small catchments. The swing of response direction, which lies in the predominance between ~~spatial heterogeneity~~area and ~~hillslope hydraulics~~L/G, needs further clarification, particularly for regional recession assessment under climate changes. Incorrect response direction from landscape structure would lead to considerable bias inference.

1 Introduction

25 Streamflow recession, the falling segment of hydrograph, reflects a rainfall-runoff process ~~in the falling segment of hydrograph~~and interaction among different runoffs during ~~the~~a rainstorm. ~~Recession is~~Therefore, recession, associated with runoff paths within landscape ~~and,~~ is particularly critical for baseflow estimation (Palmroth et al., 2010). Previous studies analyzed aggregated long-term data to retrieve recession parameters (e.g., Brutsaert and Nieber, 1977), but parameters from individual events can elucidate the recession characteristics of catchments (Jachens et al., 2020) and shed insight into the
30 sensitivity of catchments to rainstorms ~~that provides valuable information~~, which is informative for water resource

management ~~under rainfall intensification~~. Therefore, recent studies have shifted to investigate recessions from individual events (Biswal and Nagesh Kumar, 2014; Jachens et al., 2020). ~~It is crucial because the frequency and intensity of 10-year return period rainfall will increase 1.7 times and 14%, respectively (under global warming level of 2 °C, by the Intergovernmental Panel on Climate Change, Seneviratne et al., in press).~~

35 A power-law relationship between streamflow declines (streamflow rate Q recesses with a timestep t) with streamflow rates ($-dQ/dt = $ ~~aQ^b~~$\hat{a}Q^b$) can describe the recession characteristics at the catchment scale~~, since~~ (Brutsaert and Nieber ~~(,~~ 1977~~),~~ ~~henceforth referred~~). Parameter $\hat{a}$ approximates to ~~as B&N. Here,~~ the ~~coefficient a refers to~~ recession rate~~, and exponent~~ but is influenced by the unit of flow and b (see section 2.2.2), and parameter b represents the nonlinearity of storage. ~~Both recession~~Recession parameters ~~depend on hydraulic properties (e.g., hydraulic conductivity and soil porosity),~~are often linked

40 to the aquifer geometries, landscape ~~structure~~, and ~~rainstorms~~spatial heterogeneity. Since the aquifer in various landscape units (e.g., hillslope, riparian, stream) exhibits different hydraulic properties~~,~~ and landscape structure, which presents the geometry of catchments and aggregates catchment hydraulic properties, apparently reflects various recession parameters. ~~For example, recession rate, a,~~In theory, parameter $\hat{a}$ has a positive correlation with drainage density (~~Brutsaert and Nieber, 1977; Zecharias and Brutsaert, 1988) and~~ total stream length ~~(Bogaart et al., 2016),~~/drainage area) and aquifer slopes but ~~has~~ a negative

45 correlation ~~to flow-path length~~ with aquifer depths, aquifer heterogeneity (of conductivity) (e.g., Brutsaert and Nieber, 1977; Rupp and Selker, 2006) and ~~flow-path height (Bogaart et al., 2016; Karlsen et al., 2019). On the other hand, nonlinearity, b,~~inter-hillslope heterogeneity (of celerity) (Harman et al., 2009). Parameter b increases with ~~catchment area (Clark et al., 2009; McMillan et al., 2014)~~the number of streams (Biswal and ~~hillslope height (Karlsen et al., 2019). Although most literature indicated that landscape structure controls~~Marani, 2010), the ~~general or seasonal pattern of recession, few studies

50 investigated~~heterogeneity of the ~~role of landscape on recession characteristics with various rainstorms.~~aquifer (Rupp and Selker, 2006) and the inter-hillslope (Harman et al., 2009), yet decrease with the total stream length (Biswal and Marani, 2010).

~~The influence of rainstorms on recession parameters is complicated and inconsistent. Several empirical studies found a positive or independent relationship between recession rate and rainfall amount (Bogaart et al., 2016) streamflow rate (Santos et al., 2019), whereas a theoretical work found that the increasing steady-state recharge rate could either enhance or reduce~~

55 ~~recession rate, depending on the spatial heterogeneity (Harman et al., 2009). On the other hand, rainfall amount corresponded negatively (Shaw, 2016) or insensitively to nonlinearity (Biswal and Marani, 2010; Brutsaert and Nieber, 1977; Dralle et al., 2017), but antecedent wetness was positive (Harman et al., 2009; Jachens et al., 2020). The various responses from literature~~Theoretical works also have illustrated the temporal dependence of recession parameters on the groundwater table, recharge, and storage. From the perspective of temporal variability, parameter $\hat{a}$ is negatively correlated to the initial

60 groundwater table (h_0) under unsaturated conditions and renders a slightly positive correlation under saturated conditions ($h_0 > B\tan\phi$, where B is aquifer length and is ϕ aquifer angle, Rupp and Selker, 2006). A large recharge rate also reduces parameter $\hat{a}$, particularly in homogenous catchments (Harman et al., 2009). On the other hand, hydraulic theories indicate that b decreases from 3.0 to 1.5 during the transition from early to late recession, as the groundwater is vertically sourced from different hydraulic properties in wet conditions (e.g., Rupp and Selker, 2006). The spatial heterogeneity theory demonstrates that b only

65 slightly increases with the wet antecedent condition (Harman et al., 2009). However, the drainage network theory indicates that b increases/decreases with storage while reaches in downstream are contributed by more/fewer subsurface storages (Biswal and Nagesh Kumar, 2013). The various responses among theories implying the control of landscape structure and rainfall amount on recession in different regions should be improved.

The compilation of pervious empirical recession works (summarized in Table 1 and S1) demonstrated that most studies
70 elucidated the recession parameters at long-term scale, and the relationships between recession parameters against landscape, landcover, and soil were inconsistent. For example, empirical recession parameters have inconsistent responses to several physiographic variables (drainage area, drainage density, water bodies coverage, and surface saturated conductivity), implying that different landscape regimes may have distinct recession responses. Additionally, most inter-event studies just analyzed the single parameter ($\hat{a}$) that decreases with the catchment wetness, which ignores the temporal variability of b. Only Biswal
75 and Nagesh Kumar (2013) found the different directions of b response to peak flow, but which landscape variables would control the direction is still unclear. This compilation indicated that rare studies focused on the subtropical region and the variability of recession parameters at event scale.

This study investigated the recession parameters along with different magnitude of rainstorms (e.g. typhoons) on steep landscape in hope to identify the interactive role of rainfall and physiographic variables in recession. Specifically, we derived
80 the recession coefficient and nonlinearity in 19 mountainous catchments (drainage area varies between 77–2,089 km^2) across Taiwan with multiyear records of hourly streamflow (291 events in total). Due to frequent tropical cyclones (alias: typhoon) and mountainous landscapes, Taiwan's ~~river~~rivers lead to short water travel time and limit water retention capacity in catchments (Lee et al., 2020). Most typhoon rainwater falls in summer and elevates water level dramatically but diminishes quickly within 2-3 days (Huang et al., 2012). Here, the following questions are addressed: (1) What are the recession
85 characteristics of typhoon events in subtropical mountainous catchments? (2) How do rainfall and landscape variables affect recession parameters in different landscape regimes? (3) In what way do landscape variables regulate the response of nonlinearity to rainfall? We documented the spatial patterns of recession parameters in Taiwan (Sect. 3) and then discussed how the recession behaviors change in different landscape settings (Sect. 4). Finally, we proposed a hypothesis: landscape structure could swing recession responses to rainstorms. Understanding the recession behaviors after typhoons are vital to
90 water resource management, particularly when global warming likely increases the frequency and magnitude of flood and drought (Shiu et al., 2012; Huang et al., 2014).

~~This study investigated the recession parameters along with the different magnitude of typhoons on steep landscape in the hope of identifying the interactive role of climatic and physiographic variables in recession. Specifically, we derived the recession rate and nonlinearity in 19 mountainous catchments (drainage area varies between 77–2,089 km² across Taiwan~~
95 ~~with multiyear records of hourly streamflow (260 catchment events in total). The following questions are addressed: (1) what are the recession characteristics in subtropical mountainous catchments? (2) how do climatic and physiographic variables affect recession parameters? We documented the spatial patterns of recession characteristics in Taiwan (Sect. 3) and then~~

3

2 Material and methods

2.1 Study area

Taiwan is geographically located at the juncture between the Eurasian and Philippine tectonic plates and climatologically located at the corridor of typhoons. The active mountain belt with frequent typhoons shapes steep and fractured landscapes with verdant forests. The mean annual rainfall is about 2,510 mm, and approx. 40% of annual rainfall is brought by typhoons in a few days. The lowest mean annual temperature is approx. 4°C in montane regions and 22°C in plain regions. In this mountainous island, the uplifting elevation (0–4,000 m) within a short horizontal distance (~75 km) shows the steepness of thesteep terrain feature (Huang et al., 2016). Specifically, the drainage area of most catchments is smaller than ~500 km^2 and stream lengths are less than ~55 km, indicating a short water travel time. The basic catchment descriptions of landscape variables could refer to Table S1.

S2. Land cover inventories from the Taiwan Ministry of the Interior (www.moi.gov.tw) were reclassified from the original 13 categories into three major categories; namely, water, (C_W), forest, (C_F), agriculture, (C_A), and others for each catchment. The landscape metric describesdescribed by the landscape variables which were retrieved from the digital elevation model (DEM) with 20m resolution and referred to Table S2. The specific variables and their definitions in of landscape variables are below: A is the metric were referred to Table S1. drainage area [L^2]; DD is the drainage density [L/L^2] defined as the ratio of total stream length to drainage area; S_m is the gradient of mainstream [-]; HI is the hypsometric integral [-]; ELO is the basin elongation [-] defined as the ratio of the diameter of the circle (same area with the basin) to basin length. Notably, the flow-path length (L),is defined as the hillslope grid point following the surface flow direction toward the channel. Flow-path length (L) is the length of this path, and flow-path height (H), and gradient (G) above the nearest channel were retrieved by the hydrology toolset in ArcGIS 10.7, which helps to discuss) is the height difference along this path. G is the flow-path gradient [-]. These flow-path metrics and the L/G are often used in transit time studies (e.g., McGuire et al., 2005), helping to describe how landscape control on streamflow recession (e.g., Zecharias and Brutsaert, 1988; Bogaart et al., 2016; Jachens et al., 2020)..

Streamflow in this steep mountainous island usually descends quickly after a considerable surge by a typhoon. Thus, hourly streamflow records are required to describe the entire streamflow recession since it only lasts a few days after peak. This study selected hourly streamflow records during 1986-2014 from the Taiwan Water Resource Agency (www.wra.gov.tw) and Tai-Power Company (www.taipower.com.tw). Only the catchments without large water division infrastructures in the upstream area and the total rainfall larger than 30 mm were used to prevent human manipulation on streamflow and guarantee the discharge rise. Based on the criteria, nineteen catchments and 260291 events were filtered for further recession analysis. Commensurate with the hourly streamflow, the hourly rainfall dataset from the Taiwan Central Weather Bureau (www.cwb.gov.tw) was introduced to Thiessen weighted method for areal rainfall estimation to the corresponding catchments.

130 The rainfall period was defined as the elapse time from 6 hr before the rising flow to the peak flow. Collectively, a hydroclimate metric of rainstorm and streamflow presented total event rainfall, duration, average and maximum rainfall intensity, total streamflow, peak flow, and ~~initial~~antecedent flow is shown in Table ~~S2~~S3.

2.2 Recession analysis

As most analyses of hydrological processes do, the water balance equation is primarily described as Eq. (1):

135 $$\frac{dS}{dt} = P - E - Q$$

(1)

where S is the storage volume within a catchment (in units of volume [L³] or depth [L]), and P, E, and Q are the rates of precipitation [L], evapotranspiration [L], and stream discharge [L³/T] or [L/T], respectively. For solving the unknown storage, which cannot be measured directly, all terms should be identified. The ~~B&N~~ formula, $Q = mS^n$ with constant m and n (Vogel

140 and Kroll, 1992), which follows Dupuit-Boussinesq equation, can be used to derive the relationship between storage and stream discharge. In this regard, S can be replaced by Q to infer the storage changes. During the recession period, P and E are relatively small compared to Q, and then the following equation is derived to represent the recession behaviors within a catchment.

$$-\frac{dQ}{dt} = nm^{\frac{1}{n}}Q^{\frac{2n-1}{n}} = ~~aQ^b~~\hat{a}Q^b$$

145 (2)

where ~~a~~$\hat{a}$ and b are constants derived from the Q-S relation. In this study, the stream discharge has been normalized by drainage area, and the unit of Q, $\hat{a}$ and b is [mm/h], [h⁻¹ (mm/h)¹⁻ᵇ] and [-], respectively. This power-law form between $-dQ/dt$ and Q indicates that the rate of streamflow decline is highly relevant to Q during the recession and has been widely plotted as "recession plot" (Kirchner, 2009). This plot enables the analysis of streamflow recessions ~~collectively~~aggregatedly or event-

150 independently and facilitates the derivation of storage–outflow relationships (Stölzle et al., 2013). Although the ~~B&N~~power-law formula and recession plot are widely used for describing the recession behavior, the ~~calculation~~retrieval procedures of recession extraction and parameter estimation are diverse due to different practical operations. For example, Stölzle et al. (2013) compared three ~~recession~~ extraction methods of recession segment in conjunction with their corresponding parameter estimations and all possible combinations. They found that recession characteristics like recession time ($1/a$) varied over 1–2

155 orders of magnitude, yet exponent b differed rather narrowly. Their results suggested that the recession characteristics derived with different procedures have only limited comparability and highlight the distinctiveness of individual procedures due to different purposes and philosophies. Dralle et al. (2017) also agreed with the above statement but they found that the relationship between $\hat{a}$ and antecedent wetness were sensitive to the length of data. Despite the differences among the procedures, applying the same procedure to a regional extent still captures the recession characteristics. The following

160 subsections present the procedures used for extraction and parameter estimation.

5

2.2.1 Recession segment extraction

In the extraction procedure, two concerns should be addressed: (1) distinguishing between the early and late recession stage, and (2) elimination of the unexpectedly positive increases in the recession. The early-stage (containing preceding storm and surface flow) and the late stage of recession (only dominated by base flow) are indistinguishable and usually determined subjectively based on different purposes. Some studies empirically excluded the early-stage recession from eliminating the influence of quick flow (e.g., Brutsaert, 2008; Vogel and Kroll, 1992). Some other studies used a threshold for the minimum length in extraction procedures from 2- to 10-days (e.g., Mendoza et al., 2003; Vogel and Kroll, 1992). ~~Since the whole recession segment represents the mixing recession behavior from quick and base flow interactively, we used peak flow as the beginning of the recession period.~~ For eliminating unexpectedly positive increases in recession, several approaches have been proposed as well, for example, smoothing the hydrograph (Vogel and Kroll, 1992), discarding the segment directly (Brutsaert, 2008; Kirchner, 2009), and breaking-and-rejoining the recession segments (Millares et al., 2009). Each strategy has its advantages and disadvantages; smoothing the hydrograph could not completely erase the bulge caused by precipitation; discarding the segment would lose part of recession events. Although breaking-and-rejoining the recession, too, disturbs the original streamflow records, the method maintains a better integral of a recession event.

~~This study focused on the entire streamflow recession and used the complete~~ The specific procedure of recession segment~~.~~ used in this study was described below. First, the recession evolution by typhoons is our main concern and thus we selected the whole recession ~~period starting~~segment from the peak flow of the individual rainstorm. The whole recession segment represents the mixing of quick and base flow interactively. Later, we screened and broke down the hydrograph as an abrupt bulge emerged, erased the positive streamflow increases, and concatenated the remaining segments. This elimination procedure is quite similar to the master recession curve on a long-term scale (Millares et al., 2009). Third, data points corresponding to extremely low streamflow ($Q < 0.1$ mm h^{-1}) or recession ($-dQ/dt < 0.01$ mm h^{-2}) were excluded, due to the undetectable change in recession. Forth, rainfall events with an unreasonable ratio of total flow to total rainfall ($Q/P > 1.1$ or $Q/P < 0.1$) were also excluded. Ultimately, a total of 298 rainstorms were selected for further parameter estimation.

2.2.2 Parameter fitting

~~All extracted recession segments can be plotted on~~ Generally, the recession plot ($-dQ/dt$ vs Q) is widely used for estimation of ~~B&N~~recession parameters. ~~Several~~But, several fitting methods have been proposed due to different philosophies in the literature. ~~First, it fits~~One is to fit with the lower envelope of the point-cloud (Brutsaert and Nieber, 1977) since the evapotranspiration effect in a recession would lead to a higher value of $-dQ/dt$. Taking the lower envelope can prevent the evapotranspiration effect. ~~Secondly, it fits~~Another one is to fit with the entire point-cloud (Brutsaert, 2005; Vogel and Kroll, 1992) as subsoil heterogeneity may overshadow the evapotranspiration effect in larger or steeper catchments (Brutsaert, 2005). ~~Thirdly, it fits~~The other is to fit with the binned means weighted by the square of the standard error of each binned mean (Kirchner, 2009) because the lower values of $-dQ/dt$ could be affected by the measurement errors in the streamflow observation.

Recently, a virtual experiment study suggested ~~that it is unsuitable to represent a general picture through fitting with a group of data clouds (aggregated dataset) because the preceding flow can be superimposed on the event flow, resulting in underestimation of nonlinearity (Jachens et al., 2020). In contrast, fitting with individual recession segments can~~to fit with individual recession segments in order to capture the recession characteristics and offer an opportunity for exploring the impacts of rainstorm properties ~~on recession.~~. Because a group of data clouds (aggregated dataset) might result in underestimation of nonlinearity (Jachens et al., 2020). We, therefore, used each recession segment and fitted it with the ~~B&N formula~~ power-law recession individually. ~~Notably, the ordinary least square method is used to obtain estimates of parameter~~ a ~~and~~ b, ~~but the two parameters are interactively dependent, particularly when the number of points is huge.~~

The specific parameter estimation for the retrieved recession segment was described below. Firstly, low-flow record correction: the same low flows appear frequently due to the detection limit of instruments and result in a series of zero value of $-dQ/dt$ which affects parameter estimation, particularly in b. We applied the exponential time step method (Roques et al., 2017) here to reduce the bias, in which the time step of the moving window exponentially increases along the recession. The extended sampling period could avoid the occurrence of zero values of $-dQ/dt$. Secondly, the decorrelation method: another important concern of parameter estimation in recession is the dependence between a and b, which blurs the interpretation of parameters. Therefore, we applied decorrelation method which assumes that the observed flow Q consists of a scale-free flow $\hat{Q}$ and a constant k $(Q = k\hat{Q})$. Thus, the power law formula can be rewritten as $-dQ/dt = ak^{b-1}\hat{Q}^{b}$, where a is scale-free recession coefficient [h^{-1}]. For correcting $\hat{a}$ to a, the observed flow Q was divided by a constant Q_0 (ideally equal to $1/k$, see detail in Dralle et al., 2015). After the decorrelation process, the number of catchments with a high correlation between a and b ($R^2 >$ 0.1) decreased from 9 to 2. Finally, events with low goodness of fit ($R^2 < 0.5$) were discarded. Ultimately, each watershed had 5 to 26 events (total is 291, see Table S3) selected for exploring the landscape and rainstorm effects, of which events were not necessarily the same rainstorm.

3. Results

3.1. Recession parameters from individual and point-cloud fit

After proceeding with the mentioned analysis onto this dataset, we demonstrated the recession plots of W9, W5, ~~W8,~~ and ~~W18~~W8 in Fig. 2. The three catchments have distinct differences in landscape, particularly in drainage area and L/G (ratio of median flow-path length to median flow-path gradient to stream~~) and~~ ELO ~~(elongation), seeing)~~, see Table ~~1~~S2. Catchment ~~W8~~W9 has a ~~higher~~ L/G ~~(1109)~~larger A and ~~elongated shape (low~~ ELO~~=0.73), whereas W18~~lower L/G, W5 has a lower L/GA and ~~large~~ ELO, ~~indicating an oval shape.~~lower L/G, and W8 has a smaller A, but higher L/G. In descending order, the ranking of median recession ~~rates~~b is catchment ~~W8, W18, and W5. As for recession exponents, the mean~~W9 (2.34), W5 (1.96), and ~~median nonlinearity of W8~~W8 (1.63). The point-cloud derived b are 1.~~47~~45 (W9), 1.37(W5), and ~~1.60, respectively. The three median recession rates~~0.88(W8), showing all point-cloud b are ~~higher~~smaller than ~~the corresponding mean recession rates that indicate the three distribution of nonlinearity, b, are right-skewed~~median ones (Fig. 2c). Notably, the nonlinearity decreases

7

225 with the storm magnitude in ~~W5 and~~ W8, yet, ~~W5 presents an inverse pattern~~the nonlinearity increases with the storm magnitude in W9 (Fig. 2b and 2c). The opposite responses of ~~W8~~W9 and W5/W8 to storm magnitude coincide with the difference of ~~landscape variables (e.g., *L/G*) between W8 and W5.~~drainage area. This apparent association will be explored further in the Discussion section,

Further, the frequency distributions of the fitted recession ~~rate~~coefficient and nonlinearity of the total catchment-event
230 records are shown in Figure 3a-b. ~~Rate~~Coefficient, *a*, ranges from 0.~~01~~003 to 0.~~29~~273 hr^{-1} with mean = 0.~~076~~059 hr^{-1} and median = 0.~~043~~047 hr^{-1}. The large difference between the median and mean shows a right-skewed distribution. Nonlinearity, *b*, ranges from 0.~~58~~90 to ~~3.01~~4.39 with mean = 1.~~66~~976 and median = 1.~~57~~969. The small difference between the median and mean presents an asymmetric distribution of nonlinearity. Spatial patterns of recession ~~rate~~coefficient and nonlinearity are illustrated in Fig. 3c-d. Generally, larger recession ~~rates~~coefficients are located in the southwestern plain (Fig. 3c). Those plain
235 catchments also have higher *L/G* values. Apart from this, no other distinct pattern can be found in other mountainous catchments. Conversely, the plot of recession nonlinearity presents a vague pattern (Fig. 3d), and no simple relationship could be found.

The recession parameters derived from individual segments and aggregated point-cloud data are illustrated in Fig. 4. The ~~parameters from the~~ individual segment parameters which ~~demonstrates~~demonstrate the recession responses to each event~~,~~
240 present the holistic variation, whereas the point-cloud parameters ~~from the aggregated point-cloud (~~that aggregate all recession segments in ~~the~~specific catchment~~)~~ ~~show the general recession behavior in that catchment. The median of the rate, *a*, increases from 0.033 to 0.121 with a catchment~~ are generally larger for the coefficient and smaller for the nonlinearity. Notably, when the drainage area ~~of 140 km² and decreases to about 0.016 with catchment area above~~is larger than 800 km² ~~and the interquartile ranges are pretty large in catchments with the mid-sized area between 140 (W14) and 220 km² (W12). On the other hand, the~~
245 ~~medians of *a*~~(W19), the coefficients from aggregated point-cloud get similar to the median of the individual segment. The coefficients are close to the upper limit from the aggregated point-cloud ~~fits fall in the interquartile range of the individual fit distribution, indicating that the recession rates only lightly change between the fitting methods.~~for small catchments, compared to W19. Besides, the deviations of aggregated point-cloud coefficients are distinctly larger in the small catchments. The median and interquartile of nonlinearity from individual segments are irrelative to ~~catchment~~drainage area, and the values from the
250 aggregated point-cloud are consistently lower than that from individual segments ~~except W19. Besides, about half of nonlinearity, *b*, from the aggregated point-cloud are outside the interquartile range of the distribution. Considerable difference between the two fitting methods brings about.~~ Distinct differences between coefficients and nonlinearities from the two fitting methods present the manipulation of fitting method, which results in the difficulty in comparison and inference. The details of the recession characteristics for each catchment can be referred to Table ~~S3~~S4.

255

8

3.2 Recession parameters to event ~~characteristics~~and landscape variables

The correlation coefficients of recession parameters to event-associated variables are shown in Fig. 5 and Table 1 to capture how hydrometric forcing affects recession. The total precipitation (P), duration (D), total streamflow (Q_{tot}), ~~initial~~antecedent streamflow ($Q_{ini}$$Q_{ant}$) and runoff coefficient (Q_{tot}/P) are negatively correlated to the recession ~~rate~~coefficient, a. The average precipitation intensity (I_{avg}) and peak flow (Q_p), both of which represent the ~~strength of~~rainstorm magnitude, are not significant to ~~rate,~~ a. As for initial conditions, simply defined as the 7-day antecedent precipitation, AP_{7day}, is not correlated to the ~~rate,~~ a; other lengths of AP (3-, 5-, 14-, and 30-day) also show insignificant correlation to ~~the rate, a. Collectively, Q_{ini}~~a. Notably, Q_{ant} is negatively correlated to a. Unlike recession coefficient, which strongly depends on the hydrometric variables, nonlinearity, b, is only positive to Q_{ant}. It indicated that higher antecedent flow could lead to higher nonlinearity. A little surprise is that the ~~rate, a.~~ nonlinearity is statistically negative to peak flow (Q_p), presenting the nonlinearity decreases with rainstorm magnitude. To summarize from the view of the aggregated dataset, hydrometric forcing moderately controls the coefficient and only slightly involves nonlinearity.

~~Unlike recession rate, a, which strongly depends on the hydrometric variables, nonlinearity, b, is only positive to Q_{ini}. Higher initial flow could lead to higher nonlinearity. What is surprising is that no rainfall or flow variables are associated with the nonlinearity, which contradicts the presumed thoughts and will be discussed in the next section. To summarize from the view of the aggregated dataset, hydrometric forcing moderately controls the rate and only slightly involves nonlinearity.~~

~~3.3 Recession parameters to landscape variables~~

On our 19 catchments, average height (H), length (L) and gradient (G) of flow-path are approx. ~~120m, 252m~~120 m, 252 m and 0.47, respectively (Table ~~S1). The~~S2). Basically, those flow-path associated parameters are highly dependent. Thus, we used L/G, ~~regarded~~which has been proven highly correlated to water residence time (McGuire et al., 2005; Seybold et al., 2017), as a proxy presenting the interaction of landscape and climate, is approx. 951m. Forest is the dominant landscape, and the average forest coverage is approx. 67.1% with a range between 11.8-92.1%. Notably, the catchments in the western plain are characterized by gentle gradients of flow-path, such as catchments W8, W9, W11, W12, W13, and W14. Due to the gentle landscape and higher L/G, agricultural activities are the dominant land cover in those catchments. The details of landscape variables could be referred to Table S1.

The correlations between recession parameters against event and landscape variables are illustrated in Fig. 5 and Table 1. Most landscape variables (H, L, G, L/G, DD, S_m, HI, C_W, C_F, and C_A) are significantly correlated to the ~~rate~~coefficient, particularly for the flow-path-associated ones (H, L, G, L/G, and DD). ~~Note that~~The flow-path-associated variables, such as flow-path height (H), length (L), and gradient (G), are negatively correlated to the coefficients, but positive to L/G and DD. Besides, ~~the rate~~that coefficient increases with the decrease of S_m,~~ indicating~~ shows that quick recession occurs in a ~~mainstream~~catchment with ~~a~~ gentle gradient. In contrast, the ~~rate~~coefficient increases with HI, showing a sharp recession in actively eroded catchments. Moreover, the ~~rate~~coefficient increases with C_W (fraction of water body area) and C_A (fraction of

agriculture area) and decreases with C_F (fraction of forest area). ~~Results illustrate that a~~A catchment with more water bodies and agricultural lands leads to a faster recession, yet a catchment with more forest lands could reduce the recession ~~rate~~coefficient. In short, most landscape variables are highly associated with the ~~rate~~coefficient and only a few, such as *HI* and *A* are slightly negative to the nonlinearity. Yet, putting all catchments with various landscape features together may obscure the landscape control in recession ~~rate~~coefficient and nonlinearity.

4. Discussion

4.1 Recession parameters in subtropical mountainous catchments

The range of recession ~~rate~~coefficient from our 19 catchments is 0.010 to 0.290, comparable with values in the literature, for example, 0.012 to 0.230 for Swedish catchments (Bogaart et al., 2016) and 0.015 to 0.171 for USA watersheds (Biswal and Marani, 2010). Higher median recession ~~rates~~coefficients are found in W8, W11, W12, and W14, where shorter~~,~~ and steeper-flow paths ~~and, i.e.,~~ dense drainage networks, are the main landscape features. By contrast, catchments with longer~~,~~ and gentle-flow paths ~~and sparse drainage networks~~, such as W7 and W15, have lower median recession ~~rates~~coefficients. It ~~implies~~indicates that landscape structure (e.g., drainage density and flow-path-associated variables) could affect the recession ~~rate.~~coefficient, as Table 2 shows. On the other hand, the median of recession nonlinearity, *b*, is approx. 1.6 (Fig. 3b) with a range of 0.6 to 3.0, which are also comparable with the ranges in the literature. For example, values of *b* from 0.5 to 2.1 could be found in 220 Swedish catchments with low flow data (Bogaart et al., 2016), 0.6 to 1.7 for 22 Taiwanese rivers derived from low-flow data (Yeh and Huang, 2019), and 1.5 to 3.2 for 67 USA watersheds with event data (Biswal and Marani, 2010). ~~Nonlinearity higher than 1.0 indicates non~~Non-linear storage-~~-~~outflow relationship~~, typical~~ (b is not equal to 1.0) is prevalent for most catchments worldwide. In our cases, the highest and lowest median ~~nonlinearity is~~values of *b* are found in W7 and W19, respectively. Catchment W7 with high channel slope and flow-path gradient (Table S1), presents higher non-linear storage-outflow. W19, by contrast, has the similar landscape settings with W7, but has the lowest. ~~Other~~Perhaps, other controlling factors, such as geological structure or land cover, might ~~dominate~~regulate the recession behavior (Tague and Grant, 2004).

Notably, a distinct systematic bias is found between the nonlinearity derived from individual segments and the aggregated point-cloud (Fig. 4). Smaller *b* value derived from the aggregated point-cloud than that from individual segments could be expected since the flood distribution is right-skewed; that is, large number of small cases with scarce extremes. Nonlinearity *b* derived from aggregated point-cloud is synthesized from all points, which could be altered either by the numerous small cases or the scarce extreme cases as fitting. The median from aggregated point-cloud is more or less like the way ~~in~~of the master recession curve. Jachens et al. (2020) indicated that the event properties (variation among inter-event, storm magnitude, and antecedent condition) strongly affect the parameter estimation. In this regard, it suggested that using the median from individual segments to represent the central tendency of a collection of recession segments ~~is a better way to obtain the~~

4.2 Landscape structure controls the median of recession parameters

Landscape structure aggregates catchment hydraulic properties, embodying recession parameters conceivably. On the other handTherefore, recession behaviors in a catchment cancould be interpreted from two perspectives: hillslope hydraulics and inter-hillslope heterogeneity (Harman et al., 2009), both of which are highly relevant to landscape structure, notablymight be represented by the flow-path-associated variables (e.g., H, L, G, L/G, DD in Table 1), which describe hillslope hydraulics by addressing the distance) and gradient of flow to the stream. Further, a drainage area. Notably, heterogeneity may increase with catchment area generally complicatesbecause of the heterogeneitypossibility of a hillslope and consequently increases the recession nonlinearityincluding a wider range of subsurface conditions. Two studies, for example, investigated the recession behaviors in two small forested catchments (68 km^2 in Mahurangi, New Zealand, McMillan et al., 2014 and 41 ha in Panola Mountain Research Watershed, USA, Clark et al., 2009; Harman et al., 2009) and found that recession nonlinearity increases with catchmentdrainage area because a larger area accommodates more possibility of superimposition of multiple linear reservoirs.

Correlation analysis elucidates that flow-path-associated variables (H, L, G, L/G, DD) dominate the recession rate. The southwestern catchments marked by low gradient have higher recession rates (Fig. 3c); however, in our cases, most landscape variables only have a vague correlation with the recession nonlinearity (Fig. 6a). It might be explained by: first, some of our catchments are much larger than 500 km^2, which exceeds the extent of common rainstorms (usually less than 200 km^2). In those large catchments, the limited extent of rainstorm would not inducebring about a completecomprehensive recession processresponse in the outflow hydrograph (Huang et al., 2012). Second, catchmentdrainage area cannot reflect the unknown number of aquifers (Ajami et al., 2011). Moreover, Karlsen et al. (2019) argued that the dependence of landscape variables would change with streamflow rate. Specifically, the variable, H, dominates the nonlinearity during high flow, whereas the catchmentvariable, drainage area, gains more importance during low flows. Therefore, theThe relationship between hillslope hydraulics flow-path-associated variables and spatial heterogeneity withdrainage area against recession needs to be further examined in our catchments. Besides, since catchment area could not sufficiently explain the recession behaviors (Fig. 6a), we try including flow-path-associated variables to estimate the recession parameters.

4.2.1 Landscape structure to recession ratecoefficient, *a*

In trying allThe significance of landscape variables might be altered by drainage area, which might result in an opposite recession response. Further, in our cases, catchment area could not solely and significantly explain the recession behaviors (Fig. 6a). The flow-path-associated indicesvariables were tried to correlate with catchment area, we found that the L/G ratio presentsdrainage area and an inverse relationship between L/G ratio against catchmentdrainage area emerged surprisingly (Fig. 6b). The L/G ratio is, a measure of the distribution of flow-path length over gradient at a catchment scale (McGuire et al.,

2005), ~~which~~ is highly correlated to *DD* and the topographic wetness index (Beven and Kirkby, 1979). ~~The~~Therefore, *L/G* ~~or DD, therefore, can~~is apt to present the hillslope hydraulics at a catchment scale. In ~~this regard, the~~Fig. 6b, all catchments ~~can~~could be simply classified ~~from two dimensions (Fig. 6b); namely, the heterogeneity, in which Type B to~~into three types: type A is ~~from small to~~large catchments (area > 500 km^2), B is small catchments with low L/G, and ~~the hydraulics dimension, from Type B to~~C is ~~from low to~~small catchments with high L/G. ~~Based on the classification, the~~The flow-path-associated variables (*H*, *L*, *L/G*, and DD) are ~~highly correlated to~~re-applied onto the recession parameters according to this classification (Fig. 7). As expected, the recession coefficients correlate with the flow-path-associated variables. *H* is directly linked to the water table depth under the relatively homogeneous hillslopes. Hence, steeper hillslope corresponds to permeable soils with higher *H*, leading to a deeper and longer groundwater flow system and slower drainage (Karlsen et al., 2019). The high *DD* ~~(Brutsaert and Nieber, 1977)~~ and short *L* ~~(Zecharias and Brutsaert, 1988)~~ lead to a ~~quick~~higher recession ~~rate~~coefficient due to shorter flow paths. Additionally, McGuire et al. (2005) demonstrated isotopic evidence to prove that the transit ~~times increase~~time increases with *L* in Oregon, USA. In our case, both *DD* and *L/G* (Fig. 7a-c) confirm the documented ~~relationships~~relations. Catchments with high *DD* or *L/G*, which represent a denser stream network or short-and-gentle hillslopes, have a higher recession ~~rate~~coefficient.

Appeal to existing theories, flow-path variables could be regarded as the aggregation of aquifers with various geometries, or vertical heterogeneity of aquifer (Rupp and Selker, 2006). Flow-path variables L, H, G can be the proxy of *Bcosϕ*, *Bsinϕ+Dcosϕ*, and *D/B+tanϕ*, respectively. Large B and *tanϕ* aquifers have a small coefficient *a* (Fig. 3 in Rupp and Selker, 2006, where B, D, *ϕ* indicate the length, depth, and slope of the aquifer, respectively). Our inverse relationship between *H* and *a* confirms that the hydraulic parameters vary markedly with depth (Rupp and Selker, 2006).

4.2.2 Landscape structure to recession nonlinearity, *b*

The recession nonlinearity conditionally responds to landscape structure (Fig. 7e-7h). If Type A catchments (large area with low *L/G*, gray solid dots in Fig. 7) are excluded, ~~meaning only the hydraulics dimension is considered. All~~all flow-path-associated variables become statistically significant ~~for the estimation of~~with nonlinearity. The positive relationship of *b* with *H* and *L* indicates that steeper and rougher ~~hillslopes tend to divert water to temporarily store behind blocks, leading to a~~hillslope present non-linear recession ~~behavior.~~behaviour. With the increase of flow-path, subsurface runoff has more chances of flowing through various blocks (e.g., temporarily perched groundwater). The two composite indices, *DD* and *L/G*, are negatively related to the value of *b* (Fig. 7g-h~~). Short~~), perhaps because that short-and-gentle hillslopes~~, which~~ lead to a larger saturation area ~~nearby the riparian zone as rainfall, reduce the degree of heterogeneity in drainage behavior. By contrast, lower DD characterized by longer subsurface flow systems has a higher value of b~~ (Bogaart et al., 2016; Sayama et al., 2011). The expansion of saturation area indicates the whole subsurface is getting saturated and connected and thus reduces heterogeneity. It suggested that ~~hillslope hydraulics dimension (DD and L/G)~~ ratio affects the nonlinearity significantly~~, but~~ for small

12

catchments; however, it ~~was only~~is not valid ~~within catchment size less than 500km²~~ for our large catchments, which necessitates further theory development.

4.3 Rainfall amount controls the variation of recession parameters

385 Recession behavior is a convolutional response starting ~~from rainfall amount hitting the catchments. The large deviation in a fixed catchment (Fig. 7) presented the role of rainfall amount (hydrometric variables) in recession behaviors (Biswal and Nagesh Kumar, 2014).~~as rainfall falling within catchments. Thus, we separately examined the recession parameters against hydrometric variables for the three catchment types to rule out the influences (Fig. 8). Two significant findings are: (1) the recession ~~rate~~coefficient decreases with the rainfall amount in all types; (2) the recession nonlinearity shows opposite responses

390 in Type A and ~~C~~B (Type ~~B~~C is statistically insignificant). The parameter, *b*, in heterogeneity-dominated or hydraulics-dominated catchments would increase or decrease with rainfall amount, respectively. ~~In other words, landscape structure dominates the response direction of recession~~The contrasting recession responses are further discussed in the following two sections.

4.3.1 Rainfall amount on recession ~~rate~~coefficient, *a*

395 Several empirical studies found a positive or independent relationship between ~~rate~~coefficient, *a* and streamflow; for example, Santos et al. (2019) found that higher streamflow has a larger ~~rate~~*a*, reflecting a quick recession in Switzerland catchments. In Sweden, annual rainfall variation might be independent of the ~~rate~~*a* (Bogaart et al., 2016). ~~By contrast,~~ Harman ~~et al. (2009) designed a's~~ virtual ~~experiment~~experiments demonstrated that ~~theoretically considered~~ the recession ~~response corresponding to spatially heterogeneous storages. They assumed that the flow velocities of a catchment, organized by a series of hillslope~~

400 ~~with individual linear reservoirs, can be represented by a probability density distribution (pdf, e.g., Gamma distribution). Thus, the outflow and recession parameters could be evaluated by the recharge rate convolving with instantaneous unit hydrographs. Theoretically, the recession rate~~coefficient is determined by the tension between the recharge rate ~~with~~and the spatial heterogeneity of storage and flow velocity~~.~~ (Hamann et al., 2009). In ~~this regard, increasing recharge rate could reduce the recession rate. On the other hand, recharge rate also indirectly increases flow velocity and then enhances the rate, a. Therefore,~~

405 ~~the influence of rainfall amount presents various response directions in real catchments.~~
~~Recession rate in~~ our three catchment types~~ reduces~~, recession coefficients decrease with rainfall amount (Fig. 8a-c). ~~Therefore,~~It may infer that the ~~influence of~~huge rainfall ~~amount in our catchments overwhelms~~brought by typhoons may overwhelm the effect of flow velocity, resulting in a slower recession in large rainstorms. ~~Additionally, the significant decrease in~~Interestingly, Type C ~~catchments (has a~~ higher *DD* ~~or short-and-gentle catchments) is likely because~~intercept of the rainfall-

410 *a* relationship like the theorical curve of $h_0/D=1$ (Rupp and Selker, 2006), suggesting that~~, with~~ the ~~rainfall increase,~~lower H of type C tends to be saturated ~~zones connect more water from slow reservoirs resulting in slow water drainage~~and have a quick recession.

13

4.3.2 Opposite control of rainfall on recession nonlinearity, *b*

The ~~dependence~~variation of recession nonlinearity ~~on rainfall~~among events is divergent. ~~It has been documented as insensitive, negative or positive in various literature.~~ Some studies concluded that nonlinearity, *b*, is controlled by landscape structure and is static or is insensitive to rainfall (Biswal and Marani, 2010; Brutsaert and Nieber, 1977; Dralle et al., 2017). In other studies, nonlinearity, *b*, decreases with streamflow rate on different temporal scales (Shaw and Riha, 2012; Karlsen et al., 2019; Santos et al., 2019). Although some studies even argued that the nonlinearity can change over the course of an event (Rupp and Selker, 2006; Luo et al., 2018), this study treated b as a constant and the inter-event variability is discussed as the following. In our study, nonlinearity *b* presents a positive, flat, negative relationship with rainfall in Type A, B, and C catchments, respectively (Fig. 8d-f). A possible interpretation is that the short-and-gentle catchments (Type C catchments) have a wide range of contributing area, which expands with rainfall quickly. The pervasive saturation overland flow reduces the nonlinearity of recession. ~~Besides, large rainstorms also can connect saturated zones from slow reservoirs (e.g., hillslope or low hydraulic conductivity region) and thus drain water slowly.~~With the connection of saturated zones, the large storms can activate different draining sources, mixing them downstream and result in the decrease of b (as Type C demonstrated). On the contrary, the nonlinearity, *b*, increases with the rainfall amount in Type A catchments. In large and heterogeneous catchments, the expansion of contributing area is more unsteady and complicated, and thus the nonlinearity increases with rainfall amount. The nonlinearity increases with the heterogeneity ~~of catchment properties (Harman et al., 2009).~~within a large catchment (Harman et al., 2009). The contrasting response of *b* to rainfall was only found in Biswal and Nagesh Kumar (2013), which attributed to the change in subsurface flow contributions along the channel that affect the direction response of *b*. Our study revealed that landscape structure and rainfall amount dominate the direction and magnitude of recession response, respectively. Future research direction could further consider different landscape structures into modelling the intra-event variation of *b*.

4.4 Landscape structure regulates recession patterns

The above two sections elucidate ~~that~~the role of landscape ~~structure controls the response direction of recession (the median recession parameter), whereas~~ rainfall amount ~~influences the responsive degree of~~in recession behaviors. Thus, a hypothesis ~~that~~which demonstrates the interactive regulation of landscape structure and rainfall amount on recession nonlinearity is introduced (Fig. 9). Landscape structure is considered from two dimensions in terms of spatial heterogeneity and hillslope ~~hydraulics~~hydraulic, which are, respectively, represented by drainage area and ~~*DD*~~*L/G*. While the drainage area might correlate to the number of perched storages within the catchments, the ~~*DD*~~*L/G* featured by short-and-gentle hillslope indicates that the size of contributing area ~~dominates the~~associated with runoff generation ~~mechanism~~.

Along spatial heterogeneity dimension (from Type B to A, with increasing drainage area), additional perched storages respond increasingly with rainfall amount and thus enhance the recession nonlinearity. Perched storages are inclined to occur where the hydrological conductivity abruptly decreases due to heterogeneous soil properties or geological structure. ~~Large catchments tend to~~The existence of perched storages was found in an experimental forested catchment in Taiwan by an

intensive pore water monitoring scheme (Liang, 2020). Large catchments might have more perched storages, and consequently uneven spatial rainfall activate perched storages locally, and thus, the nonlinearity increases. On the other hand, along the hillslope hydraulicsL/G dimension (from Type B to C, with increasing DD), the accumulated rainfall expands saturation zone quickly, which prefers the generation of saturation excess overland flow. With the increase of DDL/G, the runoff generation mechanism varies from unpredictable subsurface runoff to overall saturation excess overland flow, and thus decreases nonlinearity.

5. Summary

Streamflow recession, which reflects the rainfall-runoff process after rainstorms, is crucial for baseflow estimation and assessment. This study investigated the recession responses to landscape structure and rainfall amount through power-law recession from 260291 catchment events spite the power-law equation being widely used, the procedure of parameter estimation is diverse and has brought about of considerable inconsistency. For example, selecting the recession segment from peak flow might derive higher nonlinearity, and using the whole point cloud data might underestimate the nonlinearity at the event scale. The determination and selection of recession segments predominatepredominates the ratecoefficient and nonlinearity significantly and leadleads to controversy, which makes the inter-comparison among studies complicated and delivers biased inference.

Several studies have demonstrated the effect of landscape structure and rainfall amount on recession parameters, yet the results are pretty diverse. In our cases, landscape structure, mainly DD or L/G, and rainfall amount play dominant roles in estimating recession ratecoefficient. The ratecoefficient increases with the increase of DD or L/G, indicating catchments with dense networks or more short-and-gentle hillslopes would lead to a higher ratecoefficient. Surprisingly, it decreases with rainfall amount; probably the large rainfall develops saturated zones connectivity, resulting in more water from slow reservoirs and drained slowly. This conceptual interpretation or hypothesis needs further validation. The diverse response direction of nonlinearity likely depends on spatial heterogeneity (drainage area) and hillslope hydraulics (drainage density),L/G, respectively. The more heterogeneous catchments give rise to the increase in the recession nonlinearity. On the contrary, catchments with higher hillslope hydraulicsgentle slopes could expand contributing area easily, and then generate saturation overland flow pervasively and thus reduce recession nonlinearity. Conjointly, our hypothesis presents an interactive regulation of landscape structure and rainfall amount to recession. In sum, landscape structure which has different preferences of recession mechanism, and the rainfall amount tunes the magnitude of recession nonlinearity apparently. If the hypothesis is valid, two challenges should be addressed further. First, the alteration of response direction lies in the predominance between spatial heterogeneity and hillslope hydraulics.L/G necessitates theoretical validation further. Clarifying which factors could present the spatial heterogeneity and hillslope hydraulics is also an arduous task but is helpfulcrucial for recession estimation. Second, the determination of response direction is crucial to the regional recession assessment, particularly for climatic scenarios.

15

~~The~~An incorrect direction would strongly affect the inference. Validating the landscape structure control in different regions would aid in completing the understating of recession variations.

480

References

495 Ajami, H., Troch, P. A., Maddock III, T., Meixner, T., and Eastoe, C.: Quantifying mountain block recharge by means of catchment-scale storage-discharge relationships, Water Resour. Res., 47, W04504, https://doi.org/10.1029/2010WR009598, 2011.

Beven, K. J. and Kirkby, M. J.: A physically based, variable contributing area model of basin hydrology, Hydrol. Sci. J., 24, 43–69, https://doi.org/10.1080/02626667909491834, 1979.

500 Biswal, B. and Marani, M.: Geomorphological origin of recession curves, Geophys. Res. Lett., 37, L24403, https://doi.org/10.1029/2010GL045415, 2010.

Biswal, B., and Nagesh Kumar, D.: A general geomorphological recession flow model for river basins. Water Resour. Res., 49(8), 4900-4906, https://doi.org/10.1002/wrcr.20379, 2013.

Biswal, B. and Nagesh Kumar, D.: Study of dynamic behaviour of recession curves, Hydrol. Process., 28, 784–792, 505 https://doi.org/10.1002/hyp.9604, 2014.

Bogaart, P. W., Van Der Velde, Y., Lyon, S. W., and Dekker, S. C.: Streamflow recession patterns can help unravel the role of climate and humans in landscape co-evolution, Hydrol. Earth Syst. Sci., 20, 1413–1432, https://doi.org/10.5194/hess-20-1413-2016, 2016.

Brutsaert, W.: Hydrology: an introduction, Cambridge university press, https://doi.org/10.1017/CBO9780511808470, 2005.

510 Brutsaert, W.: Long-term groundwater storage trends estimated from streamflow records: Climatic perspective, Water Resour. Res., 44, W02409, https://doi.org/10.1029/2007WR006518, 2008.

Brutsaert, W. and Nieber, J. L.: Regionalized drought flow hydrographs from a mature glaciated plateau, Water Resour. Res., 13, 637–643, https://doi.org/10.1029/WR013i003p00637, 1977.

Clark, M. P., Rupp, D. E., Woods, R. A., Tromp-van Meerveld, H., Peters, N., and Freer, J.: Consistency between hydrological 515 models and field observations: linking processes at the hillslope scale to hydrological responses at the watershed scale, Hydrol. Process. Int. J., 23, 311–319, https://doi.org/10.1002/hyp.7154, 2009.

Dralle, D., Karst, N., and Thompson, S. E.: a, b careful: The challenge of scale invariance for comparative analyses in power law models of the streamflow recession. Geophys. Res. Lett., 42(21), 9285-9293, https://doi.org/10.1002/2015GL066007, 2015.

520 Dralle, D. N., Karst, N. J., Charalampous, K., Veenstra, A., and Thompson, S. E.: Event-scale power law recession analysis: quantifying methodological uncertainty, Hydrol. Earth Syst. Sci., 21, 65–81, https://doi.org/10.5194/hess-21-65-2017, 2017.

Harman, C. J., Sivapalan, M., and Kumar, P.: Power law catchment-scale recessions arising from heterogeneous linear small-scale dynamics, Water Resour. Res., 45, W09404, https://doi.org/10.1029/2008WR007392, 2009.

Huang, J.-C., Yu, C.-K., Lee, J.-Y., Cheng, L.-W., Lee, T.-Y., and Kao, S.-J.: Linking typhoon tracks and spatial rainfall 525 patterns for improving flood lead time predictions over a mesoscale mountainous watershed, Water Resour. Res., 48, W09540, https://doi.org/10.1029/2011WR011508, 2012.

Huang, J.-C., Lee, T.-Y., and Lee, J.-Y.: Observed magnified runoff response to rainfall intensification under global warming, Environmental Research Letters, 9, 034008, https://doi.org/10.1088/1748-9326/9/3/034008, 2014.

Huang, J.-C., Lee, T.-Y., Lin, T.-C., Hein, T., Lee, L.-C., Shih, Y.-T., Kao, S.-J., Shiah, F.-K., and Lin, N.-H.: Effects of different N sources on riverine DIN export and retention in a subtropical high-standing island, Taiwan, Biogeosciences, 13, 1787–1800, https://doi.org/10.5194/bg-13-1787-2016, 2016.

Jachens, E. R., Rupp, D. E., Roques, C., and Selker, J. S.: Recession analysis revisited: impacts of climate on parameter estimation, Hydrol. Earth Syst. Sci., 24, 1159–1170, https://doi.org/10.5194/hess-24-1159-2020, 2020.

Karlsen, R. H., Bishop, K., Grabs, T., Ottosson-Löfvenius, M., Laudon, H., and Seibert, J.: The role of landscape properties, storage and evapotranspiration on variability in streamflow recessions in a boreal catchment, J. Hydrol., 570, 315–328, https://doi.org/10.1016/j.jhydrol.2018.12.065, 2019.

Kirchner, J. W.: Catchments as simple dynamical systems: Catchment characterization, rainfall-runoff modeling, and doing hydrology backward, Water Resour. Res., 45, W02429, https://doi.org/10.1029/2008WR006912, 2009.

Lee, J.-Y., Shih, Y.-T., Lan, C.-Y., Lee, T.-Y., Peng, T.-R., Lee, C.-T., Huang, J.-C.: Rainstorm Magnitude Likely Regulates Event Water Fraction and Its Transit Time in Mesoscale Mountainous Catchments: Implication for Modelling Parameterization. Water, 12, 1169, https://doi.org/10.3390/w12041169, 2020.

Liang, W. L.: Dynamics of pore water pressure at the soil–bedrock interface recorded during a rainfall-induced shallow landslide in a steep natural forested headwater catchment, Taiwan. J. Hydrol., 587, 125003, https://doi.org/10.1016/j.jhydrol.2020.125003, 2020.

Luo, Z., Shen, C., Kong, J., Hua, G., Gao, X., Zhao, Z., Zhao, H., and Li, L.: Effects of unsaturated flow on hillslope recession characteristics. Water Resour. Res., 54(3), 2037-2056, https://doi.org/10.1002/2017WR022257, 2018

McGuire, K., McDonnell, J. J., Weiler, M., Kendall, C., McGlynn, B., Welker, J., and Seibert, J.: The role of topography on catchment-scale water residence time, Water Resour. Res., 41, W05002, https://doi.org/10.1029/2004WR003657, 2005.

McMillan, H., Gueguen, M., Grimon, E., Woods, R., Clark, M., and Rupp, D. E.: Spatial variability of hydrological processes and model structure diagnostics in a 50 km^2 catchment, Hydrol. Process., 28, 4896–4913, https://doi.org/10.1002/hyp.9988, 2014.

Mendoza, G. F., Steenhuis, T. S., Walter, M. T., and Parlange, J.-Y.: Estimating basin-wide hydraulic parameters of a semi-arid mountainous watershed by recession-flow analysis, J. Hydrol., 279, 57–69, https://doi.org/10.1016/S0022-1694(03)00174-4, 2003.

Millares, A., Polo, M. J., and Losada, M. A.: The hydrological response of baseflow in fractured mountain areas, Hydrol. Earth Syst. Sci., 13, 1261–1271, https://doi.org/10.5194/hess-13-1261-2009, 2009.

Palmroth, S., Katul, G. G., Hui, D., McCarthy, H. R., Jackson, R. B., and Oren, R.: Estimation of long-term basin scale evapotranspiration from streamflow time series, Water Resour. Res., 46, W10512, https://doi.org/10.1029/2009WR008838, 2010.

18

Roques, C., Rupp, D. E., and Selker, J. S.: Improved streamflow recession parameter estimation with attention to calculation of− dQ/dt. Adv. Water Resour. , 108, 29-43, https://doi.org/10.1016/j.advwatres.2017.07.013, 2017

Rupp, D. E., and Selker, J. S.: On the use of the Boussinesq equation for interpreting recession hydrographs from sloping aquifers. Water Resour. Res., 42(12), https://doi.org/10.1029/2006WR005080, 2006.

Santos, A. C., Portela, M. M., Rinaldo, A., and Schaefli, B.: Estimation of streamflow recession parameters: New insights from an analytic streamflow distribution model, Hydrol. Process., 33, 1595–1609, https://doi.org/10.1002/hyp.13425, 2019.

Sayama, T., McDonnell, J. J., Dhakal, A., and Sullivan, K.: How much water can a watershed store?, Hydrol. Process., 25, 3899–3908, https://doi.org/10.1002/hyp.8288, 2011.

Seneviratne, S.I., X. Zhang, M. Adnan, W. Badi, C. Dereczynski, A. Di Luca, S. Ghosh, I. Iskandar, J. Kossin, S. Lewis, F. Otto, I. Pinto, M. Satoh, S.M. Vicente Serrano, M. Wehner, and B. Zhou: Weather and Climate Extreme Events in a Changing Climate, in: Climate Change 2021: The Physical Science Basis. Contribution of Working Group I to the Sixth Assessment Report of the Intergovernmental Panel on Climate Change, edited by: Masson Delmotte, V., P. Zhai, A. Pirani, S.L. Connors, C. Péan, S. Berger, N. Caud, Y. Chen, L. Goldfarb, M.I. Gomis, M. Huang, K. Leitzell, E. Lonnoy, J.B.R. Matthews, T.K. Maycock, T. Waterfield, O. Yelekçi, R. Yu, and B. Zhou, Cambridge University Press. In Press.

Shaw, S. B.: Investigating the linkage between streamflow recession rates and channel network contraction in a mesoscale catchment in New York state, Hydrol. Process., 30, 479–492, https://doi.org/10.1002/hyp.10626, 2016.

Shaw, S. B. and Riha, S. J.: Examining individual recession events instead of a data cloud: Using a modified interpretation of dQ/dt–Q streamflow recession in glaciated watersheds to better inform models of low flow, J. Hydrol., 434, 46–54, https://doi.org/10.1016/j.jhydrol.2012.02.034, 2012.

Shiu, C., Liu, S. C., Fu, C., Dai, A., and Sun, Y.: How much do precipitation extremes change in a warming climate?, Geophys. Res. Lett., 39, L17707, https://doi.org/10.1029/2012GL052762, 2012.

Stölzle, M., Stahl, K., and Weiler, M.: Are streamflow recession characteristics really characteristic?, Hydrol. Earth Syst. Sci., 17, 817–828, https://doi.org/10.5194/hess-17-817-2013, 2013.

Tague, C. and Grant, G. E.: A geological framework for interpreting the low-flow regimes of Cascade streams, Willamette River Basin, Oregon, Water Resour. Res., 40, W04303, https://doi.org/10.1029/2003WR002629, 2004.

Vogel, R. M. and Kroll, C. N.: Regional geohydrologic-geomorphic relationships for the estimation of low-flow statistics, Water Resour. Res., 28, 2451–2458, https://doi.org/10.1029/92WR01007, 1992.

Yeh, H. and Huang, C.: Evaluation of basin storage–discharge sensitivity in Taiwan using low-flow recession analysis, Hydrol. Process., 33, 1434–1447, https://doi.org/10.1002/hyp.13411, 2019.

Zecharias, Y. B.Seybold, H., Rothman, D. H., and Brutsaert,Kirchner, J. W.: The influence: Climate's watermark in the geometry of basin morphology on groundwater outflow, stream networks. Geophysical Research Letters, 44(5), 2272-2280Water Resour. Res., 24, 1645–1650, https://doi.org/10.1029/WR024i010p01645, 19881002/2016GL072089, 2017.

19

~~Table 1~~

Table 1: Summary of empirical recession studies that investigated the dependence of recession parameters on environmental factors. Shade blue, red, and grey represent positive, negative, and no correlation with factors, respectively. The label of number indicates the reference number in Table S1.

Factor	Centrality of recession		Temporal variability of recession					
	Long-term		Inter-annual		Inter-seasonal		Inter-event	
	â	b	â	b	â	b	â	b
Climate/Moisture								
Annual rainfall	1, 21	1 / 21	21	21				
Maximum monthly rainfall		2						
Antecedent flow					4, 5		5, 13, 22	
Peak flow							8 / 6	19 / 19 / 8
Flow rate after peak							5, 6, 9 / 23	23
Total storage change						11		
Water table elevation					8	3		
Saturated area					8	3		
60 cm soil moisture					8	3		
Baseflow	1							
Evapotranspiration	1, 21	1 / 21			3, 12, 24	24 / 3		
Aridity index	16, 17, 21	15, 16, 17, 21						
Mean relative humidity		2						
Landscape								
Drainage area	10, 16, 20 / 1	1, 7, 16, 18, 24 / 20						
Long shape of catchment	10							
Flow path height		24						
Mean elevation		2						
Standard deviation of elevation		2						
Catchment slope	17, 24	2, 17, 24						
Coefficient of variation of slope	16	16						
Topographic wetness index		2						
Drainage density	14 / 10	14						

Subsurface flow contact time		2			
Landcover					
Reforestation			21	21	
Water management			21	21	
Plateaus coverage		13			
Young volcano rock coverage	14	14			
Forest coverage	18				
Water bodies coverage	21	16, 21, 24			
	16				
Flood attenuation due to lakes	1	1			
Soil					
Soil depth		24			
Surface hydraulic conductivity	17	21			
	18	17			
Field capacity	16	16			
Moderate infiltration rates soil		2			
Slow infiltration rates soil		2			
Playas with impermeable soils		13			
Organic matter content		2			

600 **Table 2**: Spearman correlation coefficients between logarithmic hydrometric characteristics and recession characteristics for all catchment-events (n = ~~260~~291). Values in bold are statistically significant with the 99% level of confidence (p-value< 0.01).

Variable	Meaning~~a~~	~~b~~a [hr⁻¹]	b [-]~~Meaning~~
Hydrometric			
AP_{7day} [mm]	7-day antecedent precipitation ~~0.09~~	-0.~~14~~080	0.010~~7-day antecedent precipitation~~
P [mm]	Total precipitation~~0.44~~	-0.**00524**	-0.083~~Total precipitation~~
D [hr]	Duration of precipitation~~0.38~~	-0.**07432**	-0.054~~Duration of precipitation~~
I_{avg} [mm hr⁻¹]	Averaged precipitation intensity~~0.19~~	-0.**07257**	-0.026~~Averaged precipitation intensity~~
Q_{tot} [mm]	Total streamflow~~0.52~~	-0.**02609**	-0.154~~Total streamflow~~
~~Q_{ini}~~Q_{ant} [mm]	~~0.31~~Antecedent streamflow	-0.**38339**	~~Initial streamflow~~**0.266**
Q_P [mm]	~~0.13~~Peak flow	0.**09247**	~~Peak flow~~**0.228**
Q_{tot}/P [-]	Runoff coefficient~~0.29~~	-0.**00337**	-0.097~~Runoff coefficient~~
Landscape			
H [m]	~~0.62~~Flow-path height	-0.**07491**	~~Median of flow-path height above the nearest drainage~~**0.224**
L [m]	~~0.62~~Flow-path length	-0.**13520**	~~Median of flow-path length to the nearest drainage~~**0.302**
G [-]	~~0.59~~Flow-path gradient	-0.**03453**	~~Median of flow-path gradient to the nearest drainage~~0.189
L/G [m]	~~0.60~~Ratio of flow-path length to gradient	-0.**04470**	~~Ratio of flow-path length to flow-path gradient~~ -0.181
A [km²]	~~0.05~~Drainage area	0.**19040**	~~Catchment area~~-0.095
DD [km]	Drainage density~~0.60~~	-0.**10420**	-0.217~~Drainage density~~
S_m [%]	Gradient of mainstream~~0.40~~	-0.**08318**	**0.229**~~Gradient of mainstream~~
HI [-]	Hypsometric integral~~0.45~~	-0.**23498**	**0.226**~~Hypsometric integral~~
ELO [-]	Basin elongation~~0.12~~	-0.**14209**	**0.319**~~Basin elongation~~
C_W [%]	Land cover - water bodies ~~0.36~~	-0.**08330**	-0.147~~Land cover - water bodies~~
C_F [%]	Land cover - forest~~0.39~~	-0.**08281**	0.140~~Land cover - forest~~
C_A [%]	Land cover - agriculture~~0.37~~	-0.**07268**	-0.059~~Land cover - agriculture~~
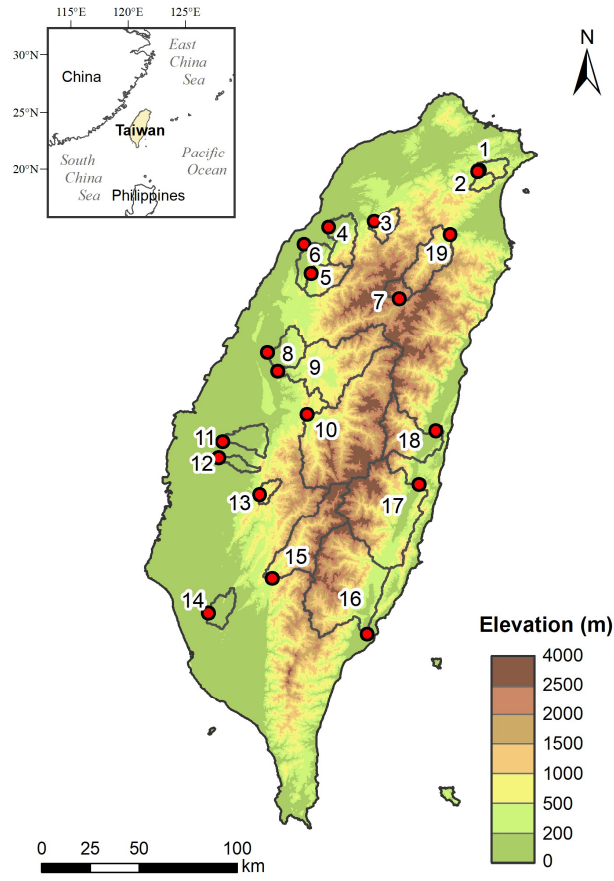
Figure 1: Topographic distribution of Taiwan and the locations of the selected catchments. The catchment ID can be referred to Table S1S2 and S2S3, in which the primary descriptions of hydrologic events and landscape variables are listed.
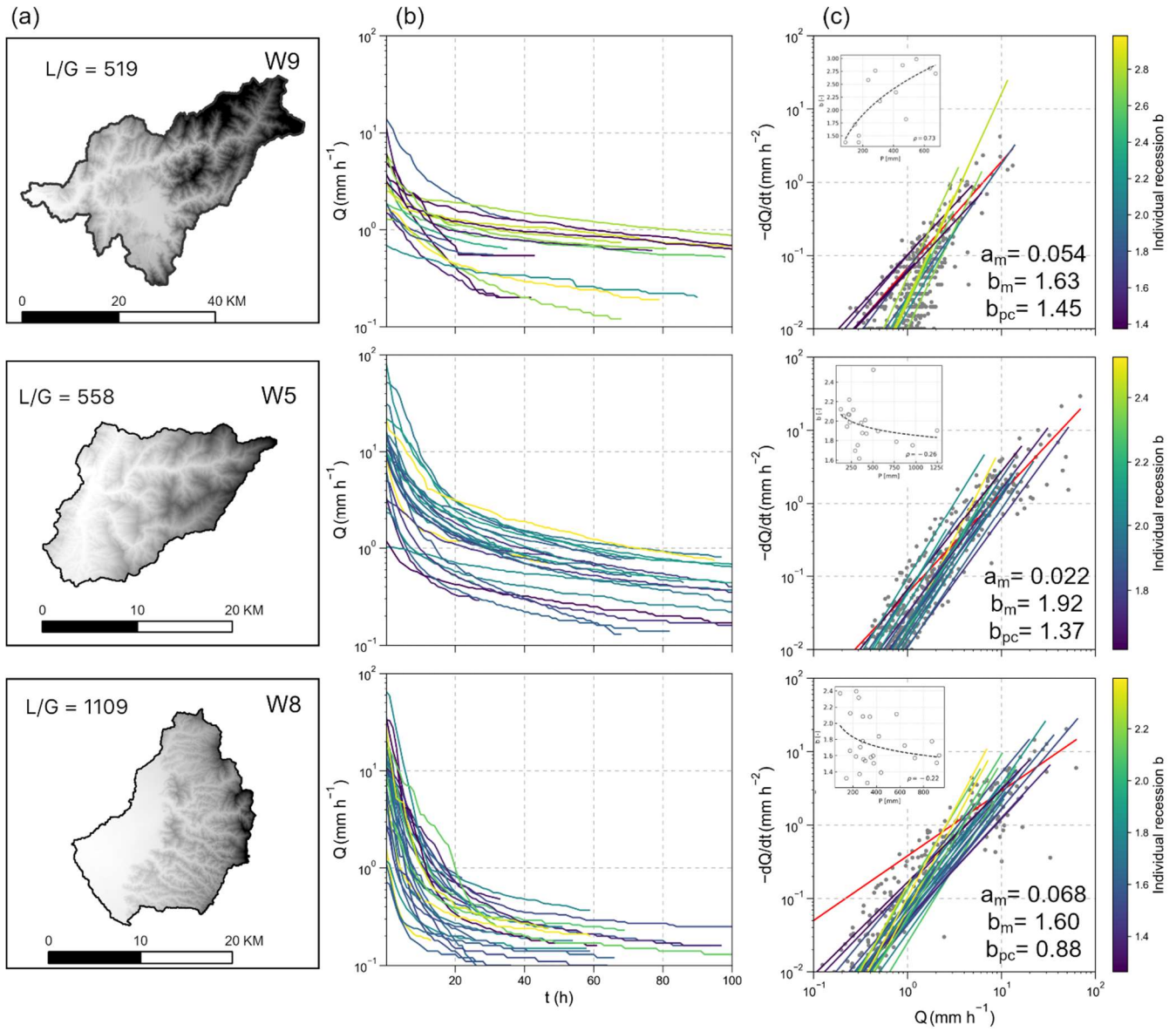
(a)

L/G=1109

W8

0   10   20 KM

L/G=519

W18

0   20   40 KM

L/G=558

W5

0   10   20 KM

(b)

$Q\,(mm\,h^{-1})$

$t\,(h)$

(c)

median a = 0.116

median a = 0.048

median a = 0.031

$-dQ/dt\,(mm\,h^{-2})$

$Q\,(mm\,h^{-1})$

Individual Exponent b
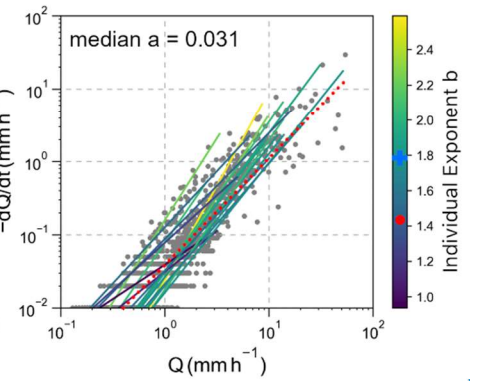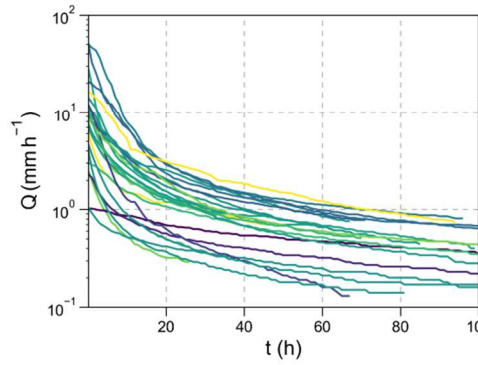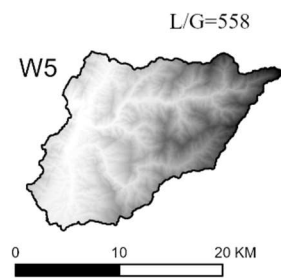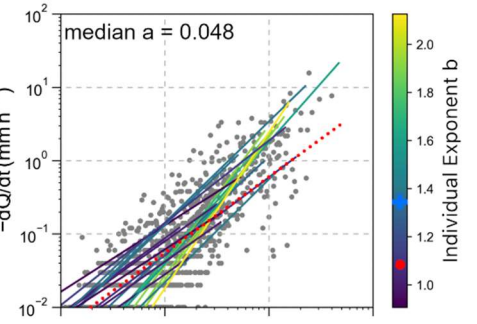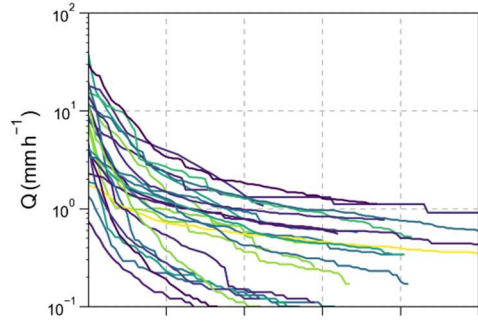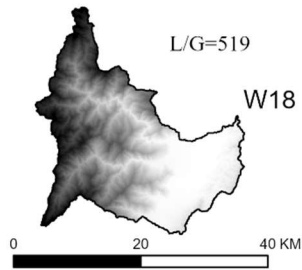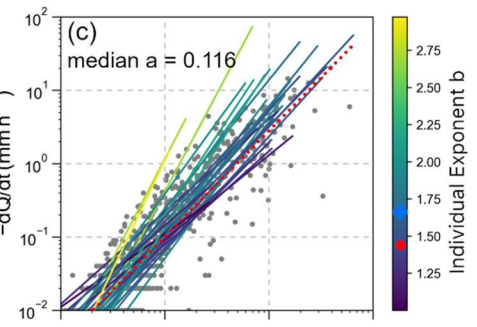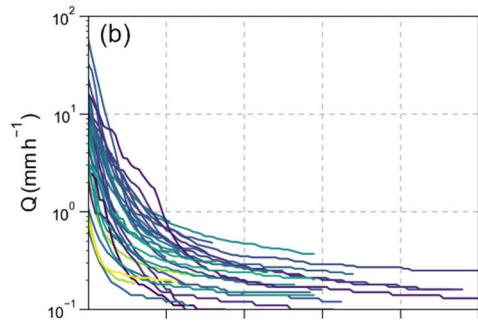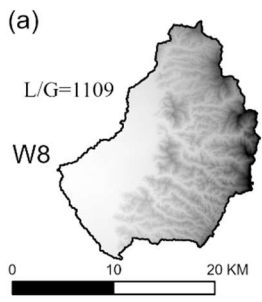
Figure 2: Landscape and recession plots for catchment ~~W8~~W9 (row 1), ~~W18~~W5 (row 2), and ~~W5~~W8 (row 3). Landscape and ~~catchment shape~~flow-path topography (L/G) are shown in column (a). The selected recession segments from different rainstorms are shown in (b). Recession plots ~~with point-cloud from~~ of all selected rainstorms are shown in column (c). The median of recession ~~coefficient~~parameter a ~~is~~ and b_m and the b_{pc} derived from the point-cloud are shown in the ~~upper-left~~lower-right corner ~~and the~~. The recession ~~exponent, b,~~ from individual segment are colored from purple to yellow with increasing value of b. ~~Note that the blue cross and red dot in the color bar represent the median and mean of the recession exponent.~~
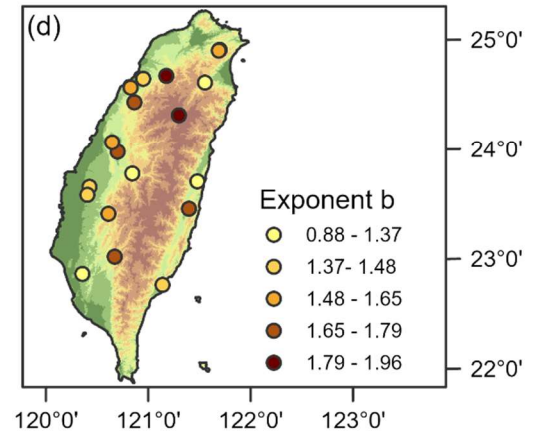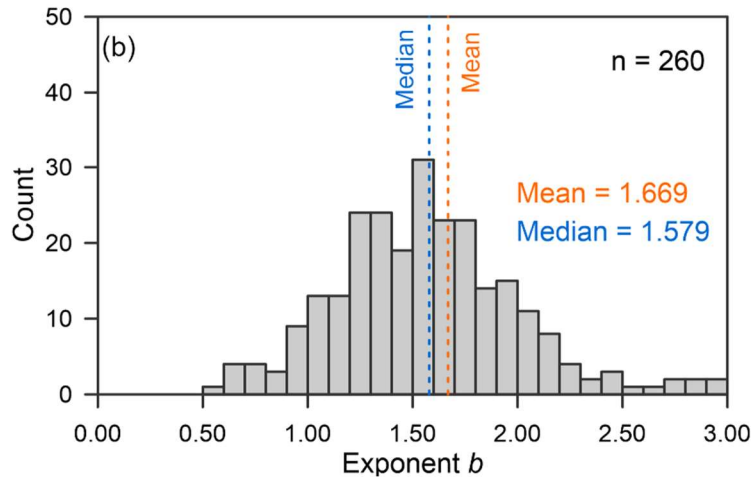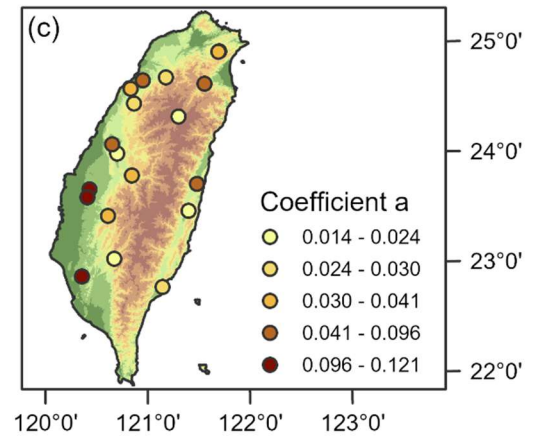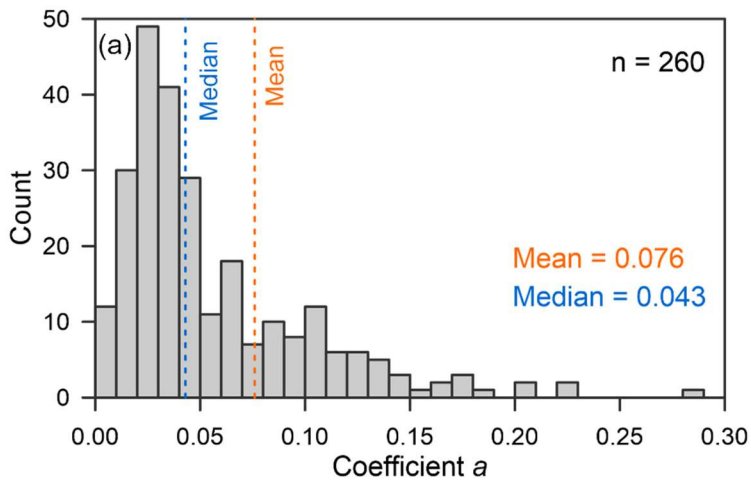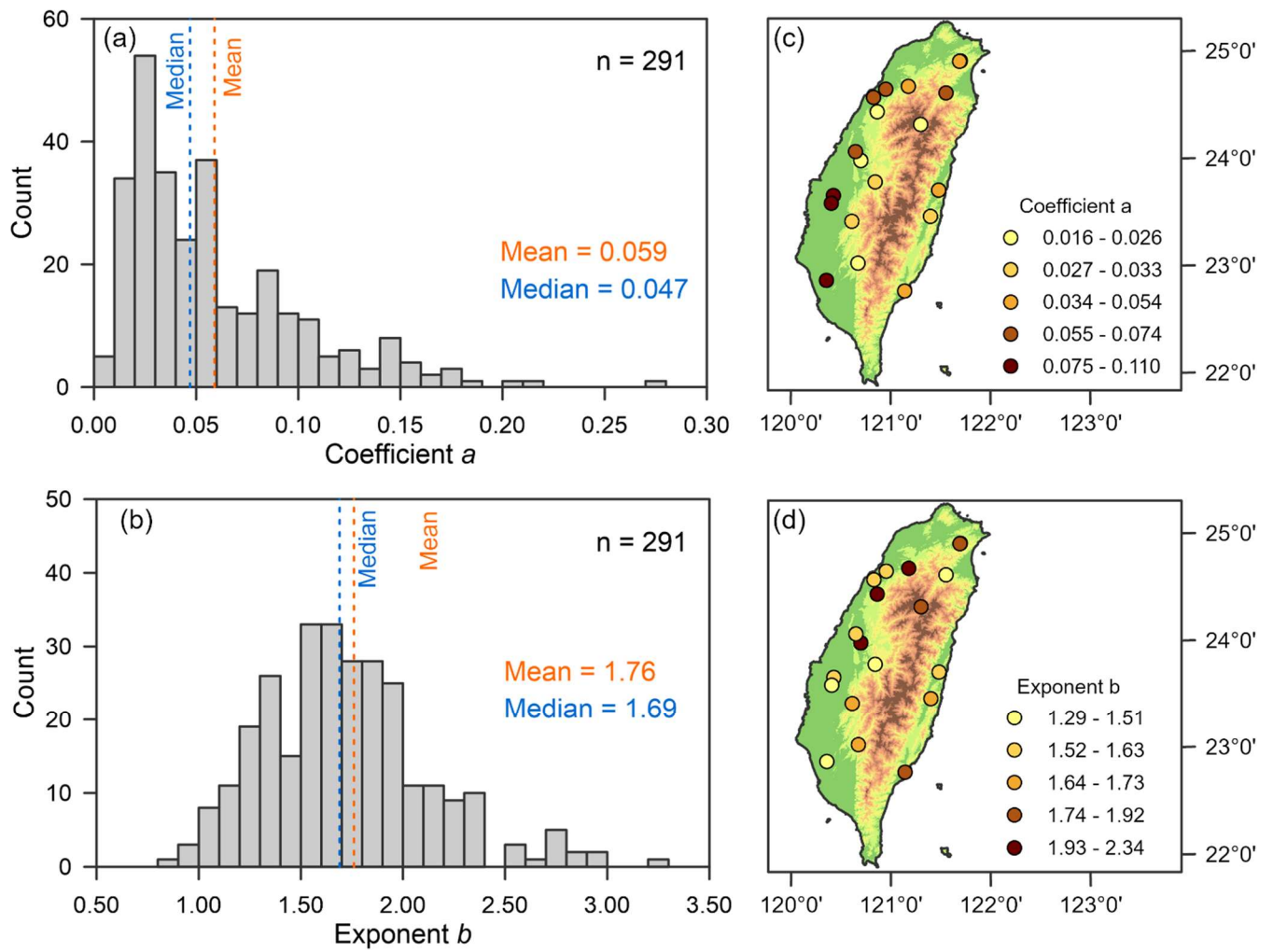
Figure 3: Distributions of recession parameter *a* (a) and *b* (b) in all catchment-events. Spatial distributions of the medians of parameter *a* (c) and *b* (d). Colors of dot represent quantiles category.
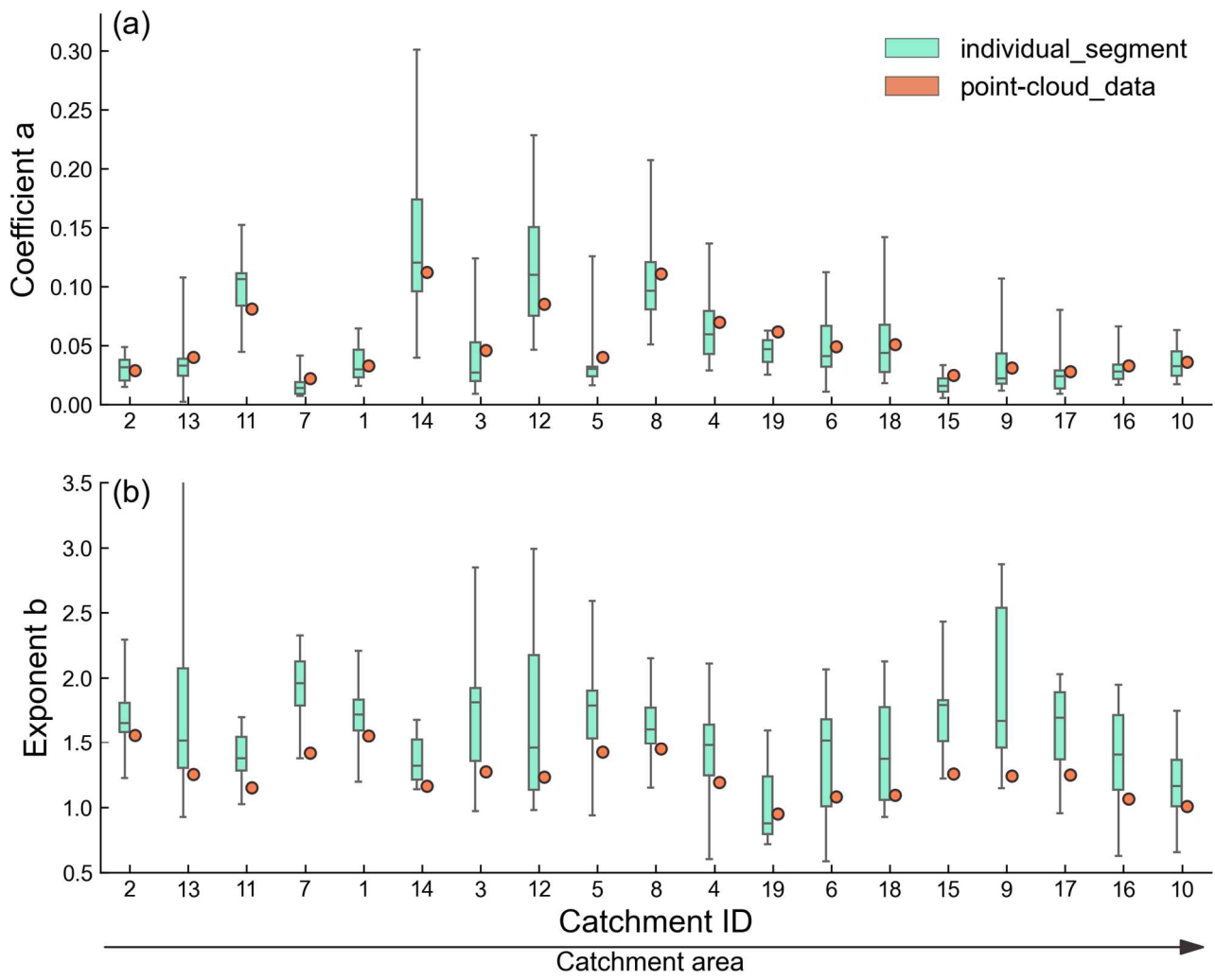
625
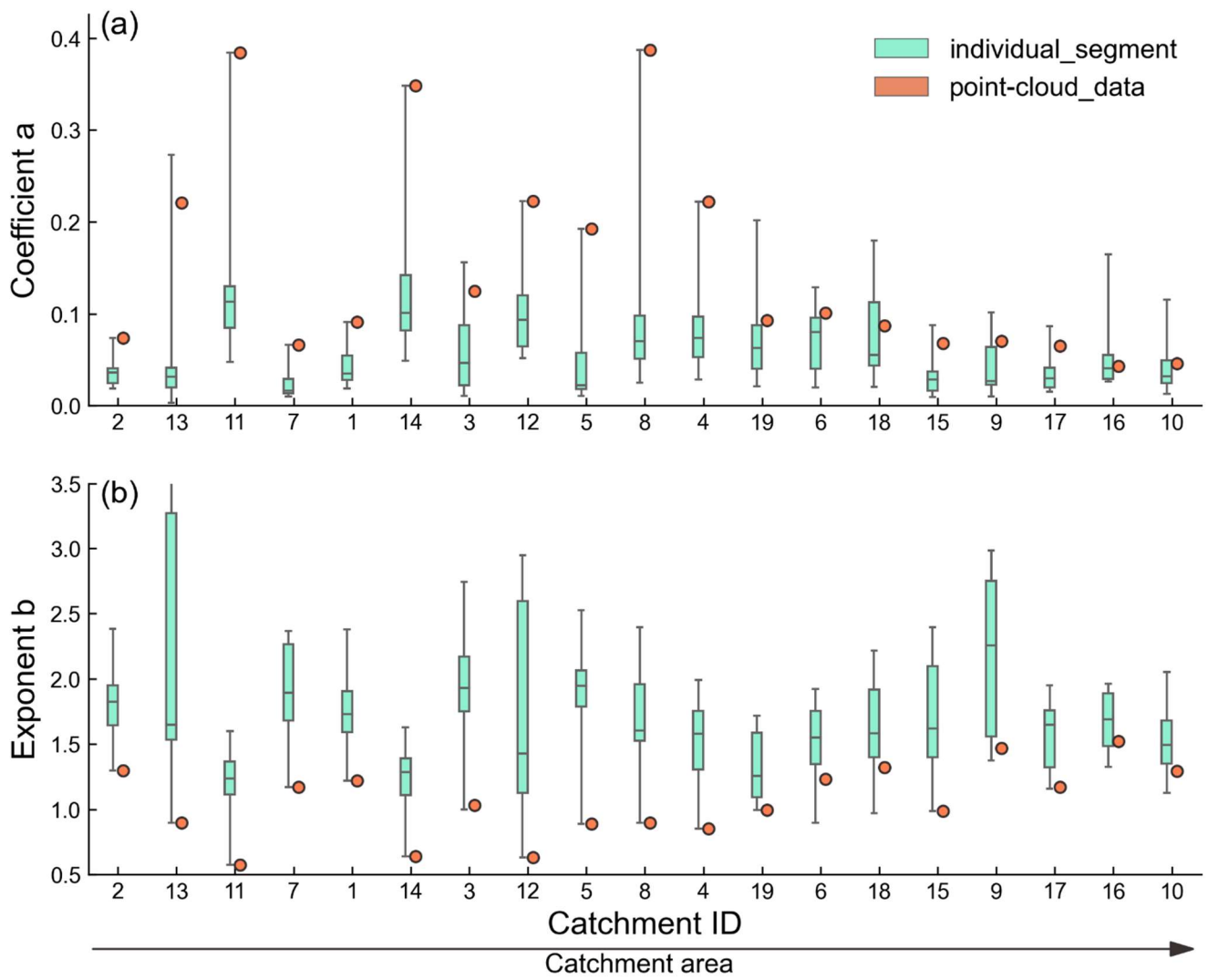
Figure 4: Boxplots of coefficient *a* (a) and exponent *b* (b) derived from individual recession segment (cyan box) and point-cloud data (orange dot). The ~~catchment~~drainage area is used in *x*-axis in ascending order. Boxes show the interquartile and data range.

630

31
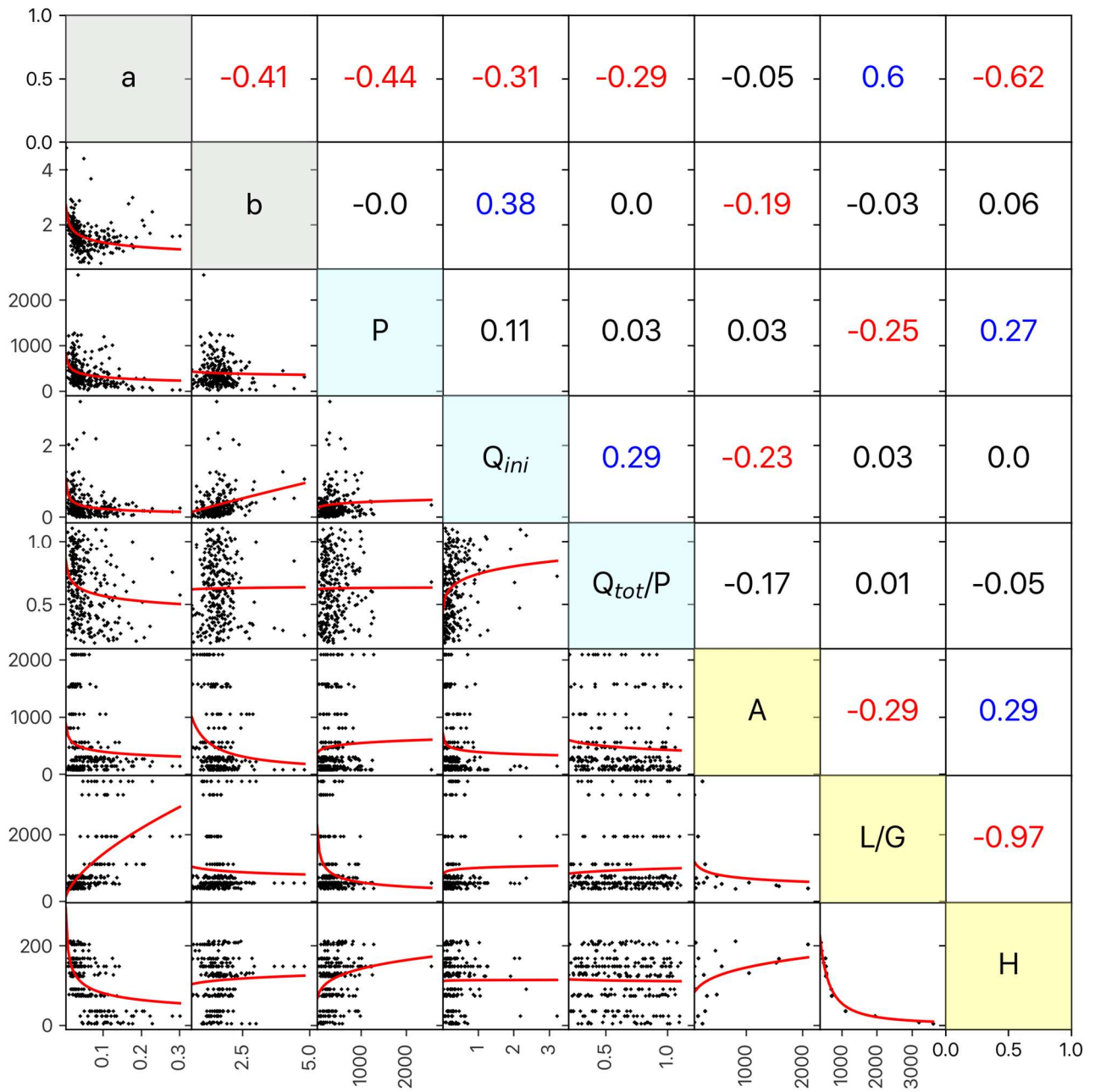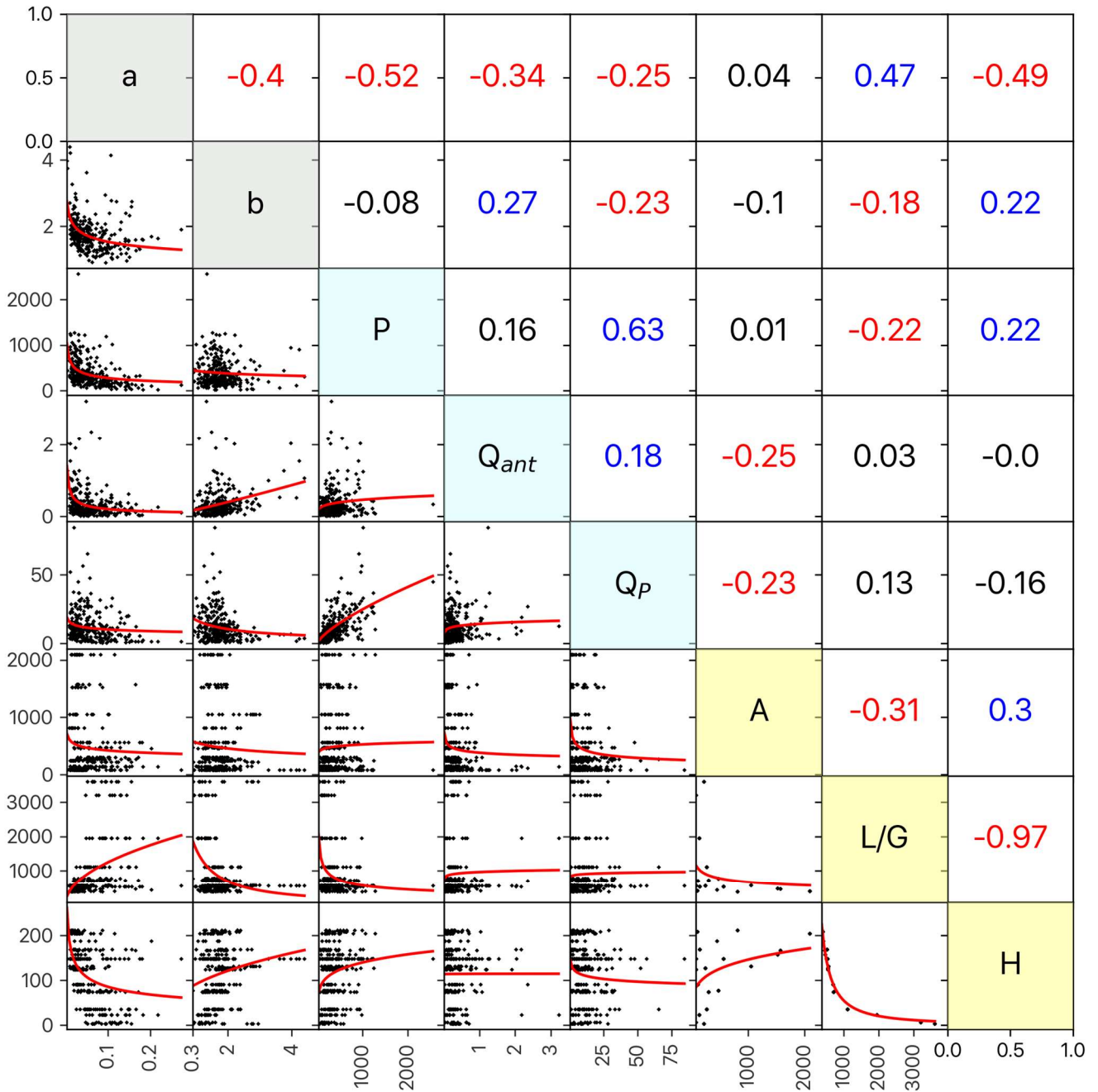
Figure 5: Recession parameter, *a* and *b* against event and landscape variables. Below diagonal: scatter plots for recession parameters with a power-fit regression (red line). Above diagonal: corresponding Spearman correlation coefficients. Values in blue and red color are positive and negative statistically significant with the ~~99~~95% level of confidence (*p*< 0.~~01~~05), respectively. Notes that all station and event are shown in this figure.

33
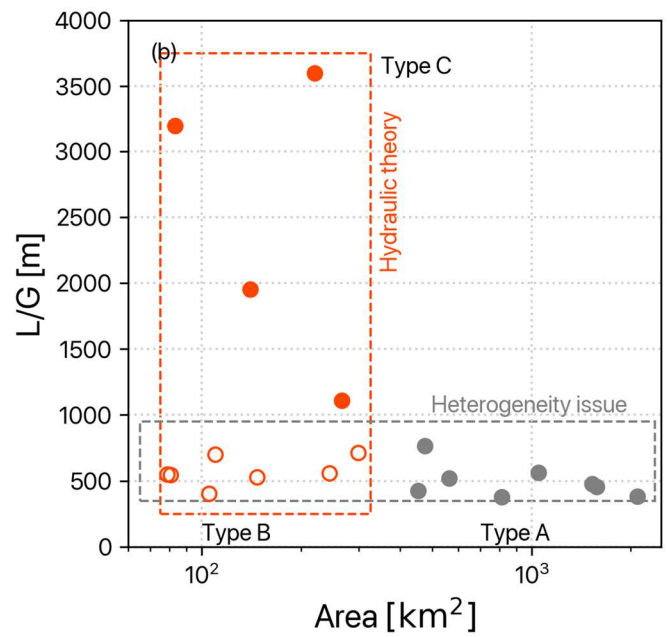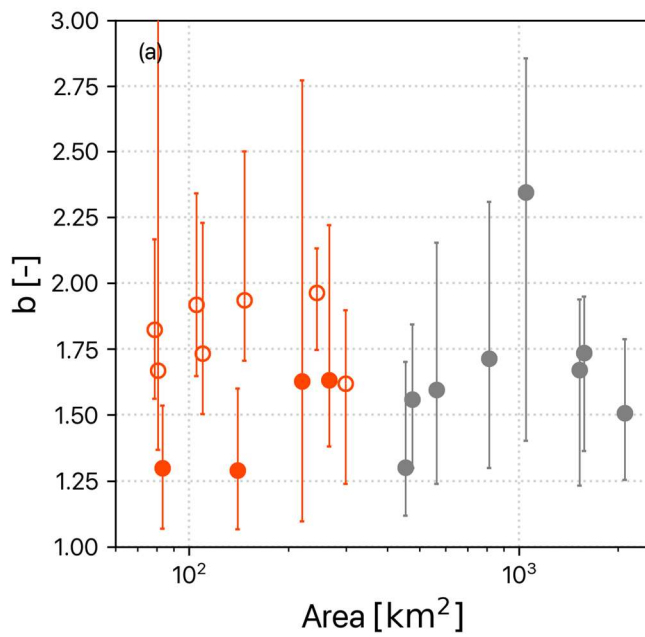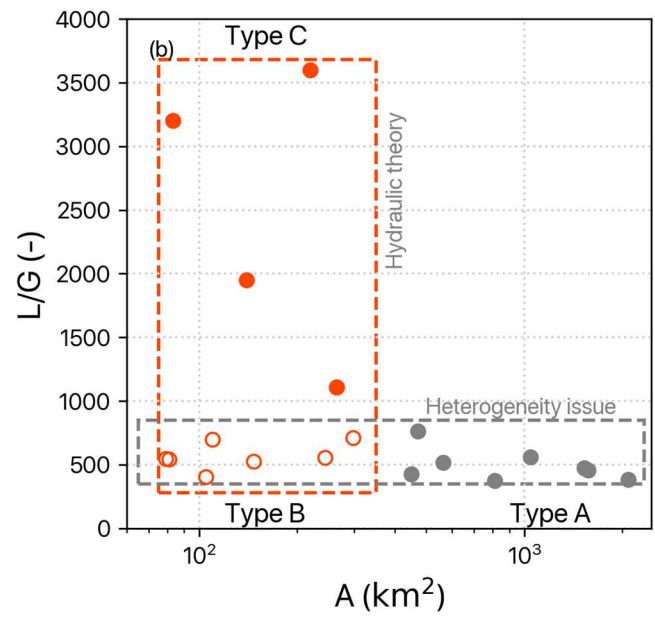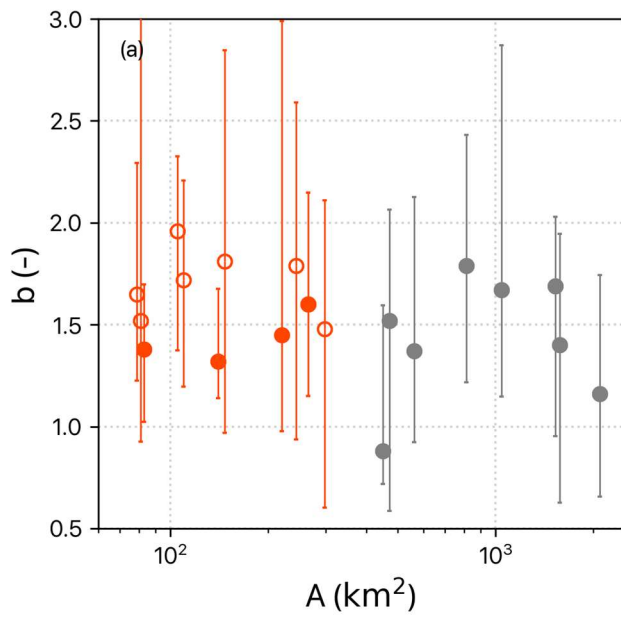
Figure 6: The relationship between ~~catchment~~drainage area and the recession exponent (a) and the flow path topography (*L*/*G*) (b). The error bar on (a) is the range of the recession exponent of each catchment. The orange and gray dots represent small and large catchments, respectively. The solid and hollow dots represent large and small L/G. The recession behaviors in small and large catchments could be explained from two perspectives in terms of hydraulic theory (orange box) and heterogeneity issues (gray box).

34
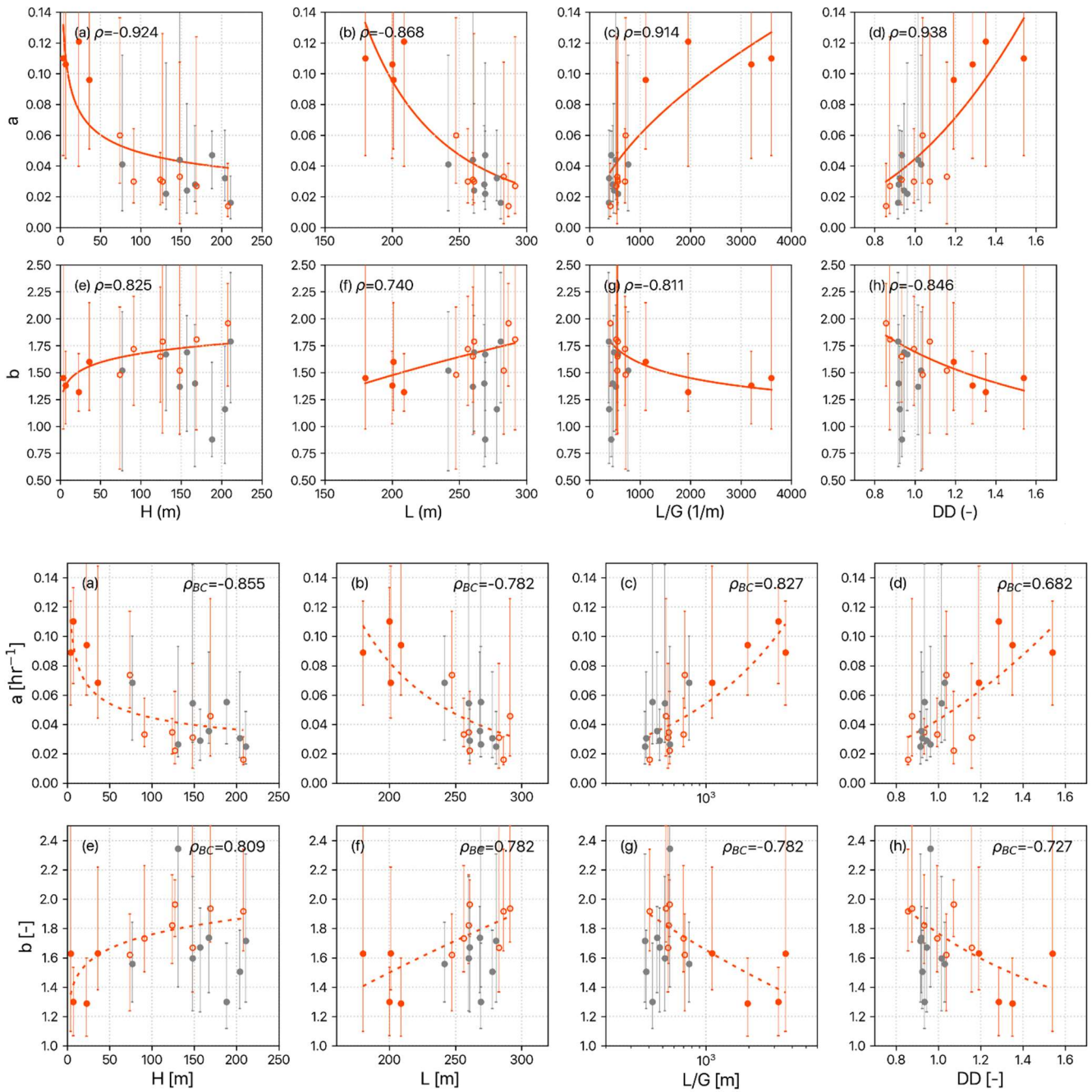
Figure 7: Scatter plots of the median and ~~the~~ range of 10th-90th percentile of recession parameters and landscape variables. ~~Orange~~gray solid, orange hollow, and ~~gray~~orange solid dots are ~~catchments of small area with high *L/G* ratio, small area with low *L/G* ratio~~Type A, B, and ~~large area~~C basin, respectively. The ~~solid~~ orange dash line is the power-law fit for small catchments~~.~~ (Type B and C), respectively. The Spearman correlation coefficient (ρ) is listed beside the annotation.
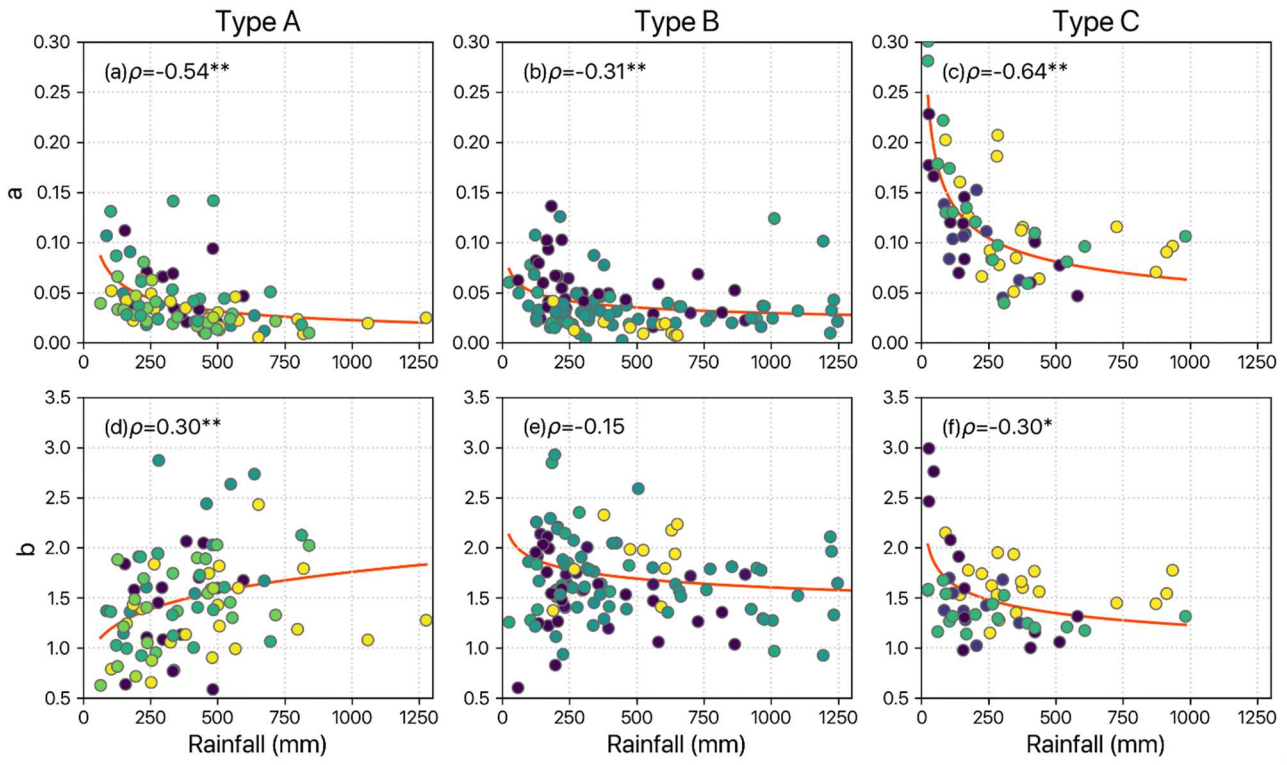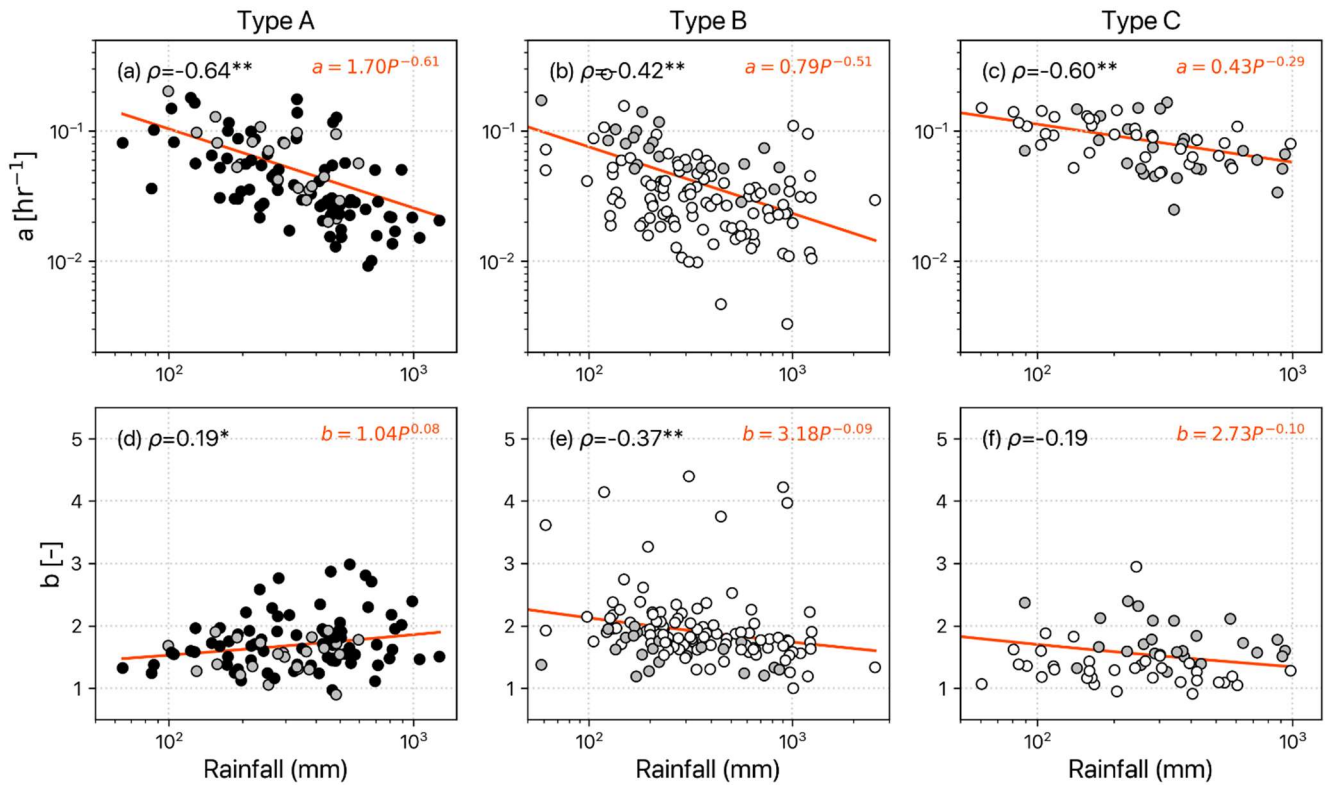
Figure 8: Scatter plots of recession parameters against total rainfall for different catchment types, corresponding to Fig. 6a. Type A is large catchments (area > 500 km^2), B is small ~~catchments~~ with low *L*/*G* ratio ~~catchments~~, and C is small ~~catchments~~ with high *L*/*G* ratio ~~catchments~~. The ~~yellow-green-blue~~black-gray-white color of dots represents the low to large L/G. The orange line is the ~~exponential~~power-law fit with spearman correlation ~~coefficient~~coefficients (* and ** means ~~95~~90% and 99% level of confidence, respectively).
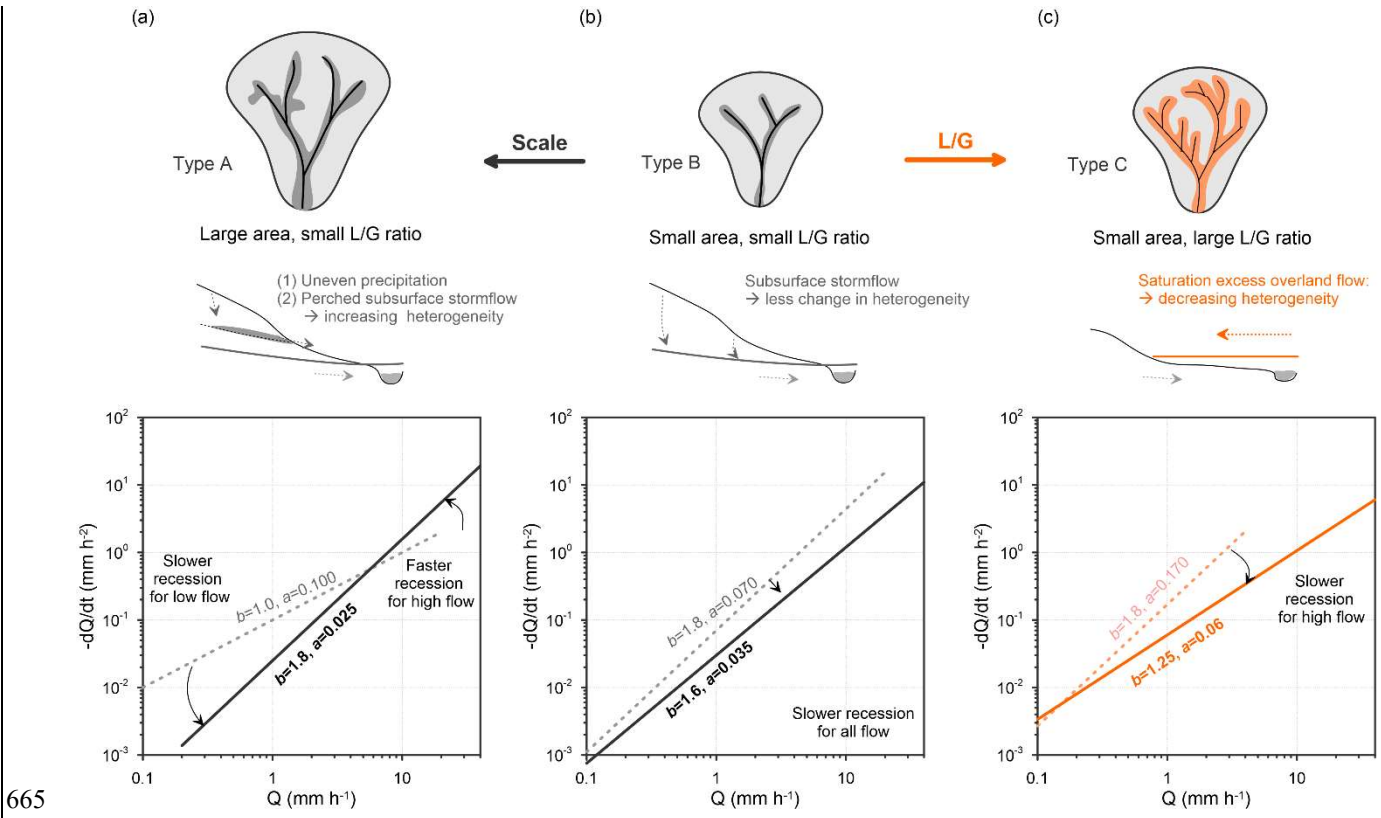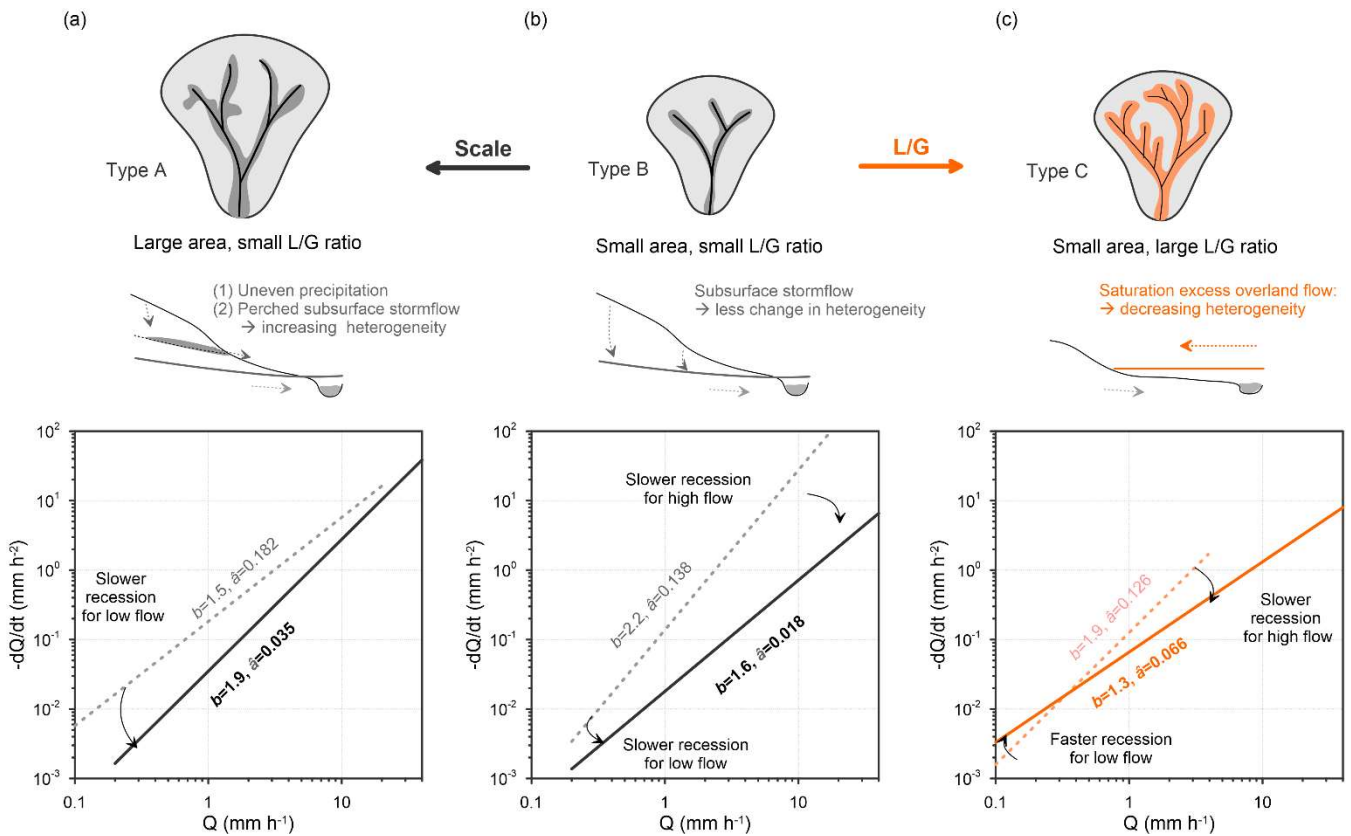
Figure 9: The conceptual diagram demonstrating the regulation of landscape variables on the direction of the rainfall-recession relationship. The top panel presents the ~~catchment~~drainage area and the stream network of three landscape types of catchment corresponding to Fig. 6b. The middle panel presents the cross-sectional valley with descriptions of drainage behavior. Here, (a) type A, large and steep slope, drains water via multiple sources of subsurface flow; (b) type B, small and steep slope, drains water via fewer sources of subsurface flow; and (c) type C, small and gentle slope, drains via the extension of the saturated zone along the riparian zone. Correspondingly, the recession plots for light (dashed line) and heavy (solid line) rainstorms with their recession parameters are presented on the bottom panel.